arXiv:1009.5994v1 [astro-ph.SR] 29 Sep 2010

A Five-year Spectroscopic and Photometric Campaign on the Prototypical α Cygni Variable and A-type Supergiant Star Deneb

N. D. Richardson[1], N. D. Morrison[2], E. E. Kryukova[2], S. J. Adelman[3]

ABSTRACT

Deneb is often considered the prototypical A–type supergiant, and is one of the visually most luminous stars in the Galaxy. A–type supergiants are potential extragalactic distance indicators, but the variability of these stars needs to be better characterized before this technique can be considered reliable. We analyzed 339 high resolution echelle spectra of Deneb obtained over the five–year span of 1997 through 2001 as well as 370 Strömgren photometric measurements obtained during the same time frame. Our spectroscopic analysis included dynamical spectra of the Hα profile, Hα equivalent widths, and radial velocities measured from Si II $\lambda\lambda$ 6347, 6371. Time-series analysis reveals no obvious cyclic behavior that proceeds through multiple observing seasons, although we found a suspected 40 day period in two, non-consecutive observing seasons. Some correlations are found between photometric and radial velocity data sets, and suggest radial pulsations at two epochs. No correlation is found between the variability of the Hα profiles and that of the radial velocities or the photometry. Lucy (1976) found evidence that Deneb was a long period single–lined spectroscopic binary star, but our data set shows no evidence for radial velocity variations caused by a binary companion.

Subject headings: stars: supergiants — stars: early-type — stars: individual (Deneb) — stars: variables: other — stars: mass loss

---

[1] Center for High Angular Resolution Astronomy, Department of Physics and Astronomy, Georgia State University, P. O. Box 4106, Atlanta, GA 30302-4106; richard-

1. Introduction

α Cygni variables are highly luminous OBA stars that exhibit low amplitude variations both in photometry ($\Delta V \lesssim 0.15$ mag; van Genderen et al. 1989) and velocity (e.g. Abt 1957). These variations are common for massive stars and are observed in most hot supergiants as well as the overluminous supergiants such as luminous blue variables. The variations have been observed in some main sequence massive stars, and the mechanism responsible for the variations has eluded theory and observers. Photometric and spectroscopic campaigns on multiple stars that span the upper H-R diagram and exhibit these variations will be crucial to understanding these variations and their source.

Deneb (α Cygni, HR 7924, HD 197345) is an early–type A supergiant (spectral type A2Iae) and is the prototype for the α–Cygni type variable stars. With a great apparent brightness and because it can be observed for most of the year at northern latitudes, Deneb can be easily studied spectroscopically with small or moderate aperture telescopes. Deneb has been one of the most studied A–type supergiants. Fath (1935) and Paddock (1935) made the first variability studies of this star, using photometry and radial velocities, respectively. Abt (1957) observed 9 supergiants, including Deneb, and showed that early and intermediate type supergiants exhibited oscillations of their atmospheres. Lucy's harmonic analysis of Deneb (1976) demonstrated that multiple oscillations were present in the atmosphere of the star. He also discovered what appeared to be a binary period in the radial velocities of Deneb. Parthasarathy and Lambert (1987) made 123 spectroscopic observations of Deneb in the near-infrared between 1977 and 1982 at McDonald Observatory. They found radial velocity variations similar to those observed by Paddock and analyzed by Lucy and claimed that the binary motion was recovered but presented no time-series analysis.

The underlying cause of the brightness and velocity variations of the α Cygni variables has been recently analyzed by a few authors. Saio et al. (2006) found that long-period oscillations in HD 163899 could be understood as g-mode pulsations that are trapped in a convection zone positioned above the H-burning shell of the star. An investigation of Deneb's variability by Gautschy (2009) gave

---

son@chara.gsu.edu

[2]Ritter Astrophysical Research Center, Department of Physics and Astronomy, University of Toledo, 2801 W. Bancroft, Toledo, OH 43606; nmorris@utnet.utoledo.edu, eallga@physics.utoledo.edu

[3]Department of Physics, The Citadel, 171 Moultrie Street, Charleston, SC 29409; adelmans@citadel.edu

evidence that Deneb also has a subphotospheric convection zone driving the variability. Cantiello et al. (2009) showed how iron convection zones above the H-burning shell could be the cause of the microturbulence and clumping in the base of the wind of hot stars. The variability for the α Cygni variables decreases in amplitude and time scale toward higher effective temperatures, and therefore these processes are easier to observe in the cooler A-type supergiants such as Deneb (e.g. Lefever et al. 2007).

Kaufer et al. (1996, 1997) examined the radial velocity variations and the Hα profile variations of Deneb and five other supergiants. They found that the radial velocities were multiperiodic and showed different periods in different observing seasons. They also found that the equivalent width of Hα exhibited multiperiodic variations and evanescent periodicities. In contrast, Morrison and Mulliss (1997) reported finding a much more active, and possibly cyclic, variability in the Hα profile. Often there are "absorption events" in which a secondary absorption component appears on the blue wing of the absorption component of the Hα profile.

Literature on photometry of Deneb is remarkably sparse, mostly due to its great apparent brightness (m_V = 1.25), combined with the fact that there are no comparison stars of similar brightness in the vicinity of Deneb. Adelman and Albayrak (1997) used HIPPARCOS observations of Deneb, as well as other early A–type supergiants, to show that these objects are small or moderate amplitude variables (a few hundredths or a tenth of a magnitude in amplitude). The light curve was not complete enough to state more than there was a period on the order of about 2 weeks, but there were most likely other effects to take into account.

It has long been known (e.g., Abt and Golson 1966) that the strength of the Hα emission in hot supergiants is correlated with the stellar luminosity. The potential of this fact for the use of these optically luminous stars as extragalactic distance indicators was greatly advanced when Kudritzki et al. (1999a,b) developed the wind momentum - luminosity relationship (WLR). However, only four A–type supergiants were in their sample, and the variability of most of these objects was neglected, with the exception of HD 92207 (A0Ia) which showed little variability in the momentum flow ($\dot{M} v_\infty$) (Kudritzki et al. 1999b). The variability of these objects needs to be investigated further in order to quantify the likely error budget in the use of this relationship. With A–type supergiants being among the brightest stars in the optical, it is important to understand this relationship between momentum flow, as derived from an Hα P Cygni profile, and the luminosity.

The variability of the Hα profile is an important diagnostic for hot supergiants in understanding the amount of clumping in the wind of these stars. If variations observed in Hα profiles were found to be repeatable, they might be attributed to corotating interaction regions in the circumstellar matter (e.g. Cranmer & Owocki 1996), which would constrain the rotation period of the star.

In this paper, we present numerous spectroscopic and photometric observations obtained during the calendar years 1997 through 2001. Such a large data set is important to understanding the complex observational variations in Deneb and other hot supergiant stars, especially in the context of the WLR. Further, variability studies in stars such as this could reveal the underlying physical mechanisms that cause the observed changes (e.g. Maeder 1980). For example, Gautschy (2009) demonstrated that some pulsational modes would be consistent with a deep convection zone for α Cygni variables.

2. Observations

339 high resolution (R = 26,000) red-yellow spectra of Deneb were obtained between 1997 March 20 and 2001 December 21 with the Ritter Observatory 1–meter telescope and fiber-fed échelle spectrograph. Details of the instrument are available in Morrison et al. (1997)[1]. For the most part, one spectrum was obtained per night, although multiple exposures were obtained on some nights. Exposure times ranged from 60 to 1200 seconds, with most being about 300-400 seconds. The average signal-to-noise ratio was around 100 for the continuum near Hα. Portions of 9 orders of echelle data were recorded, and the orders including the Hα profile and the Si II doublet at $\lambda\lambda$ 6347, 6371 are presented here. They were reduced using standard techniques for echelle spectroscopy via an IRAF[2] script.

370 differential Strömgren photometric measurements were made with the Four College Automated Photoelectric Telescope (FCAPT) during the concurrent time period of 1997 October 29 to 2001 July 2. Non-variable check (ch) and comparison (c) stars were used. Each observation consisted of a measurement of the dark count, followed by the sequence sky-ch-c-v-c-v-c-v-c-ch-sky. The light from Deneb had to be passed through a 5 magnitude neutral density filter in order to avoid detector non-linearities. The light from the comparison and check stars was not passed through the filter. The estimated error in the dif-

---

[1] A full listing of observations of Deneb at Ritter Observatory through 2006 is maintained online at http://astro1.panet.utoledo.edu/$\simeq$wwwphys/ritter/archive/Alpha-Cyg.html

[2] IRAF is distributed by the National Optical Astronomy Observatories, which are operated by the Association of Universities for Research in Astronomy, Inc., under contract with the National Science Foundation.

ferential photometry is about 0.004 magnitudes, as calculated from the standard deviation of the difference between check and comparison stars. After HD 197036 had been used as the comparison star for the first two years, with HD 198151 as the check star, it was discovered that HD 197036 is a small amplitude, long period variable star. Thus, it was replaced with HD 198151 for the remainder of these observations, and a new check star, HD 199311, was used. HD 197036 was not used for this analysis.

3. Analysis

Reductions beyond the observatory's pipeline script included removal of telluric lines, application of the heliocentric Doppler correction, and normalization to the continuum. Telluric lines were removed by means of the IRAF task `telluric`. The reference spectra were artificial templates created by mapping telluric lines in the spectra of rapidly rotating hot stars taken with the same instrumentation. Each telluric line in the template was represented by a Gaussian of the appropriate equivalent width and full width at half maximum, superimposed on a unit continuum.

When multiple exposures were taken in one night, the spectra were co-added before normalization, as spectral variability is not present on these time scales (e.g. Lucy 1976). From the continuum normalized spectra, dynamical spectra were created for the Hα profile. When observations were not available on consecutive days, the spectra were linearly interpolated for the missing observations, provided the gap was less than 10 days. The net equivalent width of Hα was measured for each of the continuum normalized spectra. The integration window was 22 Å centered on the laboratory wavelength of Hα, and the estimated errors in the measurements are less than 5% based on the techniques described by Chalabaev and Maillard (1983).

Radial velocities were measured for the Si II $\lambda\lambda$ 6347, 6371 doublet by means of a Gaussian fitted to each line. A weak Fe II line was found to be blended into the blue wing of Si II λ 6371, and was also fitted when determining the radial velocity of that line. When more than one observation was available for a single night, the radial velocity was measured for each observation; the variations were never more than 0.5 km s^{-1} over the course of a night. Observation series of stable giant stars with this spectrograph and camera generally yield standard deviations of a single measurement on the order of 0.5 km s^{-1}. Typically, the radial velocities of the two Si II lines agreed with each other to within 1 km s^{-1}, but usually to within less than 0.5 km s^{-1}.

The differential magnitudes were approximately converted to standard

Strömgren *uvby* magnitudes, using values for the comparison stars from Hauck and Mermilliod (1998). The colors $u-b$ and $b-y$ and the Strömgren indices c_1 and m_1 were calculated. Because no attempt was made to correct for any color dependence that may exist in the attenuation of the neutral density filter, and because multiple *uvby* standard stars were not used, the colors we derived for Deneb are not precisely on the standard system.

4. Results and Time-Series Analysis

4.1. Dynamical Spectra of Hα

Dynamical spectra were created for each observing season in order to explore the temporal behavior of the Hα profile. Figure 1 shows the variations of Deneb during calendar year 1997. Several strong absorption events occur on the blue wing of the P Cygni profile at intervals of approximately 40 days. We define an absorption event for Deneb by the presence of a second absorption component in the blue wing of the principal absorption component. Usually this second absorption had a velocity blueshifted less than 100 km s^{-1}. The emission component remained fairly static, with the exception of two periods of strengthening. The absorption events we observed do not show a progression to the terminal velocity, as seen in discrete absorption components (DACs) of other hot, massive stars or in the high-velocity absorption events described by Kaufer et al. (1996) in hotter supergiants such as Rigel (B8 Ia). Aufdenberg et al. (2002) found that the terminal wind speed for Deneb is 225 km s^{-1}. Neither this observing season nor subsequent observing seasons show evidence that the Hα absorption reaches the terminal wind speed. The line probably has a low optical depth at large distances from the star, due to insufficient population in the $n = 2$ level.

The cyclic-type behavior during the 1997 observing season was not repeated in the other observing seasons. The 1998 season (Figure 2) exhibits two absorption events, which are farther apart than the 40 day interval of the 1997 season. The emission feature is nearly static for that year of observations. The 1999 season (Figure 3) shows an exceptionally static Hα profile for this star, with a possible beginning of an absorption event at the end of the observing season. One absorption event is observed in 2000 (Figure 4), but showed a more rapid onset and disappearance than the other observed events in our data set. The 2001 season (Figure 5) began with a very strong absorption event, and included one smaller event around HJD 2452075-2452100. The time span of September and October of 2001 (HJD 2452160-2452240) provided an interesting event that is discussed in Section 4.2.

4.2. The High-Velocity Absorption Event of 2001

The remarkable event of late 2001 began with a quick onset of a strong emission component. The absorption component reached a larger negative velocity than had previously been observed by us or by Kaufer et al. (1996a,b, 1997). As the event subsided, we observed a quick and dramatic fading of the P Cygni emission. Such a small level of emission had not previously been observed in Deneb. Figure 6 illustrates the details of this event in line plots.

The event also showed at least two additional absorption components at some epochs, and a dynamical spectrum created by subtracting the average line profile of the time period (Figure 7) reveals that this was actually two absorption events, spaced by the same period of 40 days observed with minor events in 1997. There is a sudden onset of a highly blueshifted (~ -100 km s^{-1}) absorption that increases in strength with time. About 40 days after the onset of this event, we see a second high velocity absorption event occur. As this second event reached its maximum absorption strength, we observed an onset of absorption on the red wing of the profile. This event fits the definition of a high-velocity absorption event, given in Kaufer et al. (1996). These events are described as events, with a larger blue velocity and deeper absorption than normally observed, a similar morphology throughout the time development of the event, and no evidence of any spherical symmetry in the wind at these epochs. The high velocity absorption events are much more extreme than the "normal" absorption events described in §4.1.

4.3. Hα equivalent widths

We measured the net equivalent widths of all our Hα profiles (Table 1, available online). The errors in these net equivalent width measurements are typically 1% of the measured value as determined using the methods of Chalabaev & Maillard (1983). The Hα profile shows a P Cygni type profile, so the net equivalent width does not provide a simple measure of all the variability. Using the IRAF task `splot`, we measured the equivalent width of the emission component by trying to interpolate linearly across the base of the component. Unfortunately, this method is prone to personal error. From multiple measures from the same spectrum, we derived a typical error for the equivalent width of the Hα emission component to be 5% of the measured value. We then subtracted the emission component from the net equivalent width in order to obtain an absorption equivalent width.

We found that the net equivalent width had an average value of 1.318 Å with a standard deviation of 0.197

Å. The overall estimated strength of the absorption component(s) varied by slightly more than a factor of two ($W_{\lambda,\mathrm{H}\alpha,\mathrm{abs}}$=2.172 Å on HJD 2450999; $W_{\lambda,\mathrm{H}\alpha,\mathrm{abs}}$=1.067 Å on HJD 2450669). The absorption component was 1.616 Å with a standard deviation of the mean of 0.209 Å.

4.4. Radial Velocities and Photometry

In order to derive the systemic velocity of Deneb, we computed an unweighted average over all the observations of the Si II 6347, 6371 doublet, assuming no wind contamination of these lines. The result was -2.77 km s^{-1}, which is consistent with values derived from other studies (e.g. Lucy 1976; Parthasarathy & Lambert 1987). The radial velocity had a range of values of -10.8 to 9.1 km s^{-1}, consistent with the sum of the multiple pulsation mode amplitudes (10.44 km s^{-1}) derived by Lucy (1976).

The differential *uvby* Strömgren measurements (Table 2, available online) were averaged over all data to adopt the photometric parameters for Deneb given in Table 3. u, v, b, and y had a range of 0.09, 0.14, 0.41, and 0.19 magnitudes respectively. The colors $u-b$ and $b-y$ had a range of 0.075 and 0.081 magnitudes respectively. The Strömgren indices c_1 and m_1 were found to vary by 0.233 and 0.141 magnitudes, respectively.

4.5. Time-Series Analysis and the Binarity of Deneb

In order to verify the reliability of various time-series analysis algorithms, their output was compared to that obtained by Lucy (1976) for the data collected by Paddock (1935). A Scargle periodogram analysis (Scargle 1982) of the data from Paddock (1935) only reproduced one aspect of the analysis of Lucy (1976), the long term variability that was suspected to be binary motion of Deneb.

The confirmation of the binary nature of this prototypical supergiant would be useful for understanding the star, as well as its early evolution (including mass transfer) and estimating the current mass. We used the Scargle periodogram and the CLEAN algorithm (Roberts et al. 1987) to search our data set for the binary period, and found that the power spectrum reached a relative minimum in the period range that was suspected. As Lucy (1976) could not add other data to the data of Paddock to better constrain the orbit (Section III of his paper), and our data do not suggest any binary motion, the binary hypothesis for Deneb is not supported.

A method that is more robust for datasets containing multiple periodicities, the CLEAN algorithm was used to search for periodicities in the data sets. An analysis of the radial velocity data from Paddock (1935) produced similar results to that of Lucy (1976). The results are shown in Figure 8, where we plot the frequencies and their relative strengths found for each observing season for net Hα equivalent width, Si II radial velocities, and Strömgren y. The time-series analysis was performed on the entire data set, but because of the changing characteristics of the star, no global properties were found with a high probability of being real. If the same period were found for all three data sets, there would be some evidence for a photospheric-wind connection, but our analysis showed no evidence of this behavior. Similarly, if there were evidence for similar periods in just the photometry and radial velocities, that would provide information about pulsational behavior of the photosphere of Deneb.

4.6. Radial Pulsations

Our analysis did find some periods that were the same for the radial velocities and for the photometry during 1998 and 1999. The phased (to HJD 2450000.0) data were fitted (minimum χ^2) with a sine curve of the form

$$N = A \times \sin(2\pi(p - x_c)) + c \qquad (1)$$

where N is the parameter we are fitting (radial velocity or magnitude), p is the arbitrary phase we are solving for, A is the amplitude, x_c is a phasing offset, and c is an offset for the systemic velocity or magnitude. The period was not allowed to vary during these fits. The parameters for our photometric and radial velocity fits are given in Table 4 for the two epochs of radial pulsations and the variations are shown graphically in Figure 9. The offsets in phase between the photometry maximum and radial velocity maximum for the two periods with the highest probability of radial pulsations (epochs with strong signals that match with both the photometry and radial velocity data; the fall of 1998 ($P = 17.8$d) and the fall of 1999 ($P = 13.4$d)) are roughly $0.25P$, which strongly supports the hypothesis that Deneb was experiencing radial pulsations at these epochs.

5. Discussion

We have searched for high-velocity absorptions in a sample of B8Ia - A2 Ia supergiants that have been monitored at Ritter Observatory since 1992. Our initial results, which are shown in Table 5, begin to constrain the range of effective temperatures in which supergiant stars exhibit high-velocity absorption events. With the five years of data we have analyzed combined with the data presented in Kaufer et al. (1996), only one high velocity absorption event has been observed in Deneb. These events are thus very rare for this star. Other stars of similar properties (ν Cep[3] and 6 Cas) have not shown any signs of high velocity absorption in a long time series of observations. We can therefore conclude that Deneb is at the lower end of the range of effective temperature and luminosity ($T_{\rm eff}$ ~8500±200 K, $\log(\frac{L}{L_\odot})$ ~5.2; Aufdenberg et al. 2002) for which supergiants can exhibit high velocity absorption events.

---

[3] For ν Cep, there are numerous cases of enhanced absorption in the blue wing with maximum absorption around -100 km s^{-1} and

As discussed in Section 4.6, we found evidence for radial pulsations in the atmosphere of Deneb at two epochs during our five year investigation on this star. These pulsations were present for a few cycles and then vanished. Kaufer et al. (1997) did not find radial pulsations for Deneb, although their data may have suggested such variability. Simultaneous photometry of the star is necessary for finding the radial pulsations because the atmosphere is also unstable to many non-radial modes simultaneously. The light curves at the epochs where we found radial pulsations have an amplitude such that they cannot be easily explained with non-radial modes (see e.g. Unno et al. 1979 for a description of non-radial oscillations).

6. Conclusions and Future Work

Evidence was found for radial pulsations at two epochs during this campaign. Radial pulsations are somewhat rare in the atmosphere of Deneb, where the atmosphere is does not usally display these variations. With only two short epochs having radial pulsations, we find that Deneb displays radial pulsations ≤20% of the time. While photometry was difficult to obtain for such a bright target, it is necessary to find such behavior. A complete look at all the available data collected for this star will potentially lead to a better understanding of its interior. Gautschy (2009) has demonstrated that the variability of Deneb may be indicative of an underlying convective region for this star. Detailed analyses of the variability of a larger population of supergiants could demonstrate if these intermittent radial pulsations are normal for the population.

A 40 day period was found with absorption events in 1997 as well as in the high velocity absorption event of 2001. A similar period is reported by Kaufer et al. (1996) for the 1991 observations (Hα) of Deneb. Aufdenberg et al. (2002) derived a stellar radius of 180 $R_\odot$ and $v \sin i = \approx 25$ km s^{-1} for Deneb, which corresponds to a rotational period of 58 days. The $v \sin i$ was used in the spectral line fitting of the star, and no error bars were given, but a small increase of ≈ 10

---

edge velocity around -200 km s^{-1} as in the Kaufer et al. (1996) definition, but the equivalent width involved is small. These velocities are sometimes hard to estimate because of water line contamination and/or indistinct edges. From the Mg II profiles in the Verdugo et al. (1999) atlas, the terminal wind speed of ν Cep is lower than Deneb's by about 35 km s^{-1}, so events will be harder to distinguish for that reason.

km s^{-1} to this parameter will yield a rotational period of $\approx$ 40 days. Similarly, the radius of the star could be reduced by $\approx$ 30% to yield this period. With a poorly determined parallax ($\pi = 2.31 \pm 0.32$ mas; van Leeuwen 2007), the interferometric radius determined by Aufdenberg et al. (2002) cannot be used to constrain this parameter. Therefore, we conclude that the 40 day period is consistent with the rotation period of the star and these observations may indicate occasional coupling between the photosphere and the wind.

During each observing season, the behavior of the Hα profile was different. Therefore, long-term monitoring (over multiple seasons) is crucial to understanding the variability mechanisms of stars such as Deneb. With the extreme variability seen at the time of the high velocity absorption event in 2001, caution should be used on assigning mass-loss rates and other parameters to a single-epoch observation for Deneb and similar stars. Further work will be needed for the wind-momentum luminosity relationship (Kudritzki et al. 1999a,b) with the variability of these stars taken into account.

There is a need for observing campaigns at high spectral resolution for stars in the temperature and luminosity regime of Deneb. The high velocity absorption event we observed in 2001 is the only observed event for Deneb. High-resolution spectroscopic monitoring of Deneb at Ritter Observatory spans nearly two decades (1993 through present), and analysis of the entire data set is planned and will provide additional insights into the frequency of occurrence of high-velocity absorption events, of episodes of radial pulsation, and perhaps of other phenomena. Similar stars (in temperature and luminosity) need monitoring to see if Deneb is unique and where the temperature and luminosity boundary for high velocity absorption events is located.

We acknowledge the anonymous referee for making suggestions that improved this paper. We are grateful for the Ritter Observing team who performed the spectroscopic observations during the calendar years 1997 through 2001, especially Karen Bjorkman, Anatoly Miroshnichenko, David Knauth, Chris Mulliss, Howard Ritter, Tracy Smith, Will Fischer, Patrick Ouellette, John Wisniewski, and Josh Thomas. The spectra were reduced by Chris Mulliss, David Knauth, and John Wisniewski by means of a script written by R. C. Dempsey, and later modified by J. P. Aufdenberg. Chris Mulliss created the first dynamical spectrum of Deneb from Ritter spectra, and began this project. Amber Ferguson analyzed radial velocity standard stars which helped to understand the error associated with our measurements; she was supported by NSF-PREST. We would like to thank Observatory Technician Robert Burmeister for keeping the telescope in excellent working condition. This research has made use of the SIMBAD database, operated at CDS, Strasbourg, France. Support for E. Kryukova on this project came from the NSF–REU program. Support for Ritter Observatory during the time of the observations was provided by the Fund for Astrophysical Research and the American Astronomical Society Small Grants Program. Support for FCAPT during the time period came from NSF grant AST-0587381. Special thanks to Louis J. Boyd, George McCook, and Robert J. Dukes, Jr. for their help in keeping the FCAPT in good working order. We thank Douglas Gies (Georgia State University) for helpful discussions related to the pulsational behavior of Deneb and for some software used in Figure 7.

Facilities: Ritter Observatory, Four College Automated Photoelectric Telescope

REFERENCES

Abt, H.A., 1957, ApJ, 126, 138

Abt, H.A., & Golson, J.C. 1966, ApJ, 143, 306

Adelman, S.J. & Albayrak, B. 1997, IBVS 4541, 1

Aufdenberg, J.P. et al. 2002, ApJ, 570, 344

Barlow, M. J. & Cohen, M. 1977, ApJ, 213, 737

Cantiello, M. et al. 2009, A&A, 499, 279

Chalabaev, A. & Maillard, J.P. 1983, A&A, 127, 279

Cranmer, S. & Owocki, S. 1996, ApJ, 462, 469

Fath, E. 1935, Lick Obs. Bull., 17, 115

Gautschy, A. 2009, A&A, 498, 273

Hauck, B. & Mermilliod, M. 1998, A&AS, 129, 431

Kaufer, A. et al. 1996, A&A, 305, 887

Kaufer, A. et al. 1997, A&A, 320, 273

Kudritzki, R.P. et al. 1999a, A&A, 350, 970

Kudritzki, R.P. et al. 1999b, in IAU Colloquium, 169, 405

Lefever, K., Puls, J., Aerts, C. 2007, A&A, 463, 1093

Lucy, L. B. 1976, ApJ, 206, 499

Maeder, A. 1980, A&A, 90, 311

Markova, N., Prinja, R. K., Markov, H., Kolka, I., Morrison, N., Percy, J., Adelman, S. 2008, A&A, 487, 211

Morrison, N.D. and C.L. Mulliss. 1997, BAAS, 191, 125.04

Morrison, N.D., Knauth, D. C., Mulliss, C. L., and Lee, W. 1997, PASP, 109, 676

Paddock, G. 1935, Lick Obs. Bull., 17, 99

Parthasarathy, M. and D. Lambert. 1987, J. Astrophys. Astr., 8, 51

Roberts, D.H., J. Lehár, and J.W. Dreher. 1987, AJ, 93, 968

Saio, H., et al. 2006, ApJ, 650, 1111

Scargle, J.D. 1982, ApJ, 263, 835

van Genderen, A.M. et al. 1989, A&ASS 79, 263

van Leeuwen F. 2007, A&A 474, 653

Verdugo, E., Talavera, A., & Gómez de Castro, A.I. 1999, A&A, 346, 819

Unno, W., Osaki, Y., Ando, H., & Shibahashi, H. 1979, University of Tokyo Press, "Nonradial Oscillations of Stars"

This 2-column preprint was prepared with the AAS LaTeX macros v5.2.

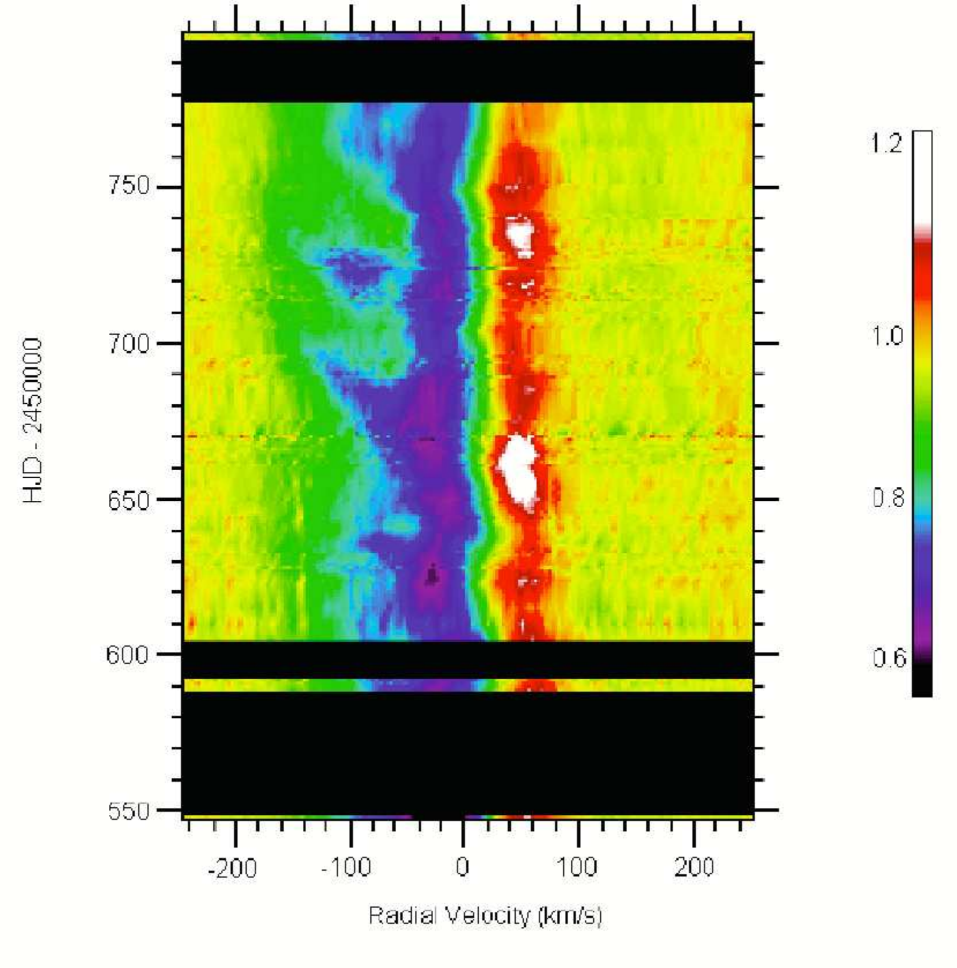

Fig. 1.— A dynamical spectrum of the Hα profile for the year 1997. There are increases in the blue wing absorption ("absorption events") near HJD 2450635, 2450675, and 2450715.

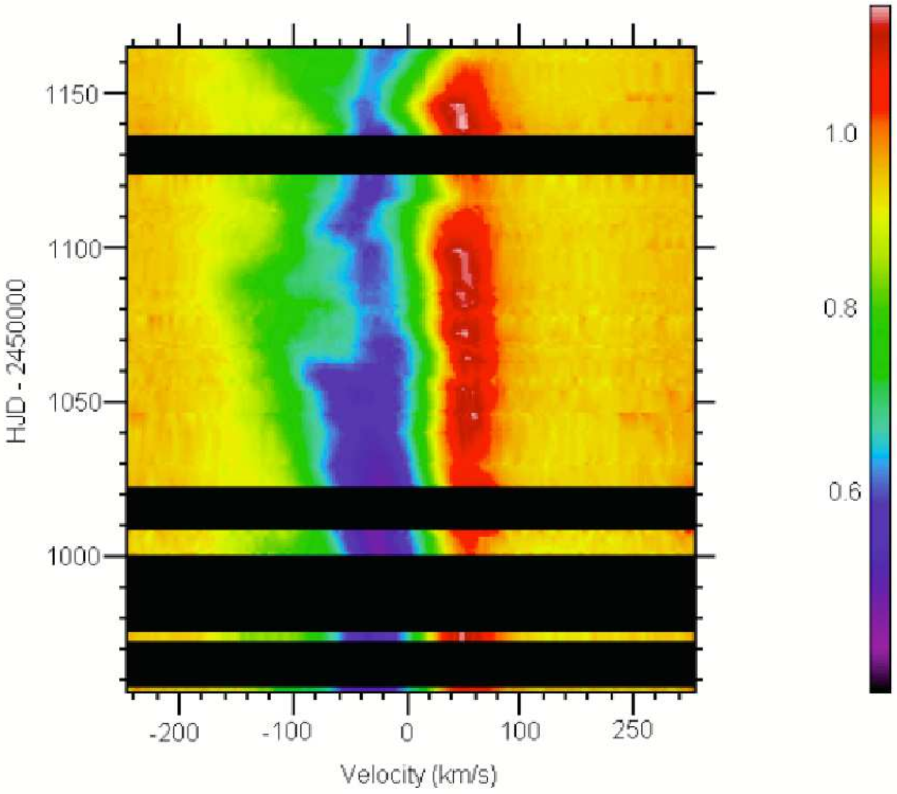

Fig. 2.— A dynamical spectrum of the Hα profile for the year 1998.

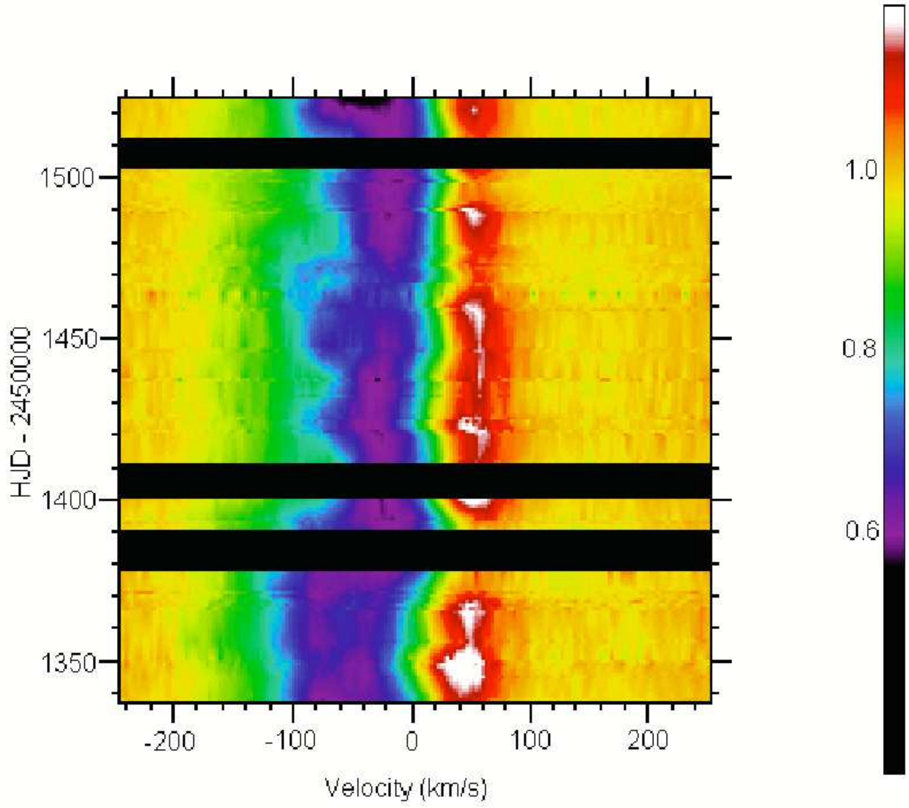

Fig. 3.— A dynamical spectrum of the Hα profile for the year 1999.

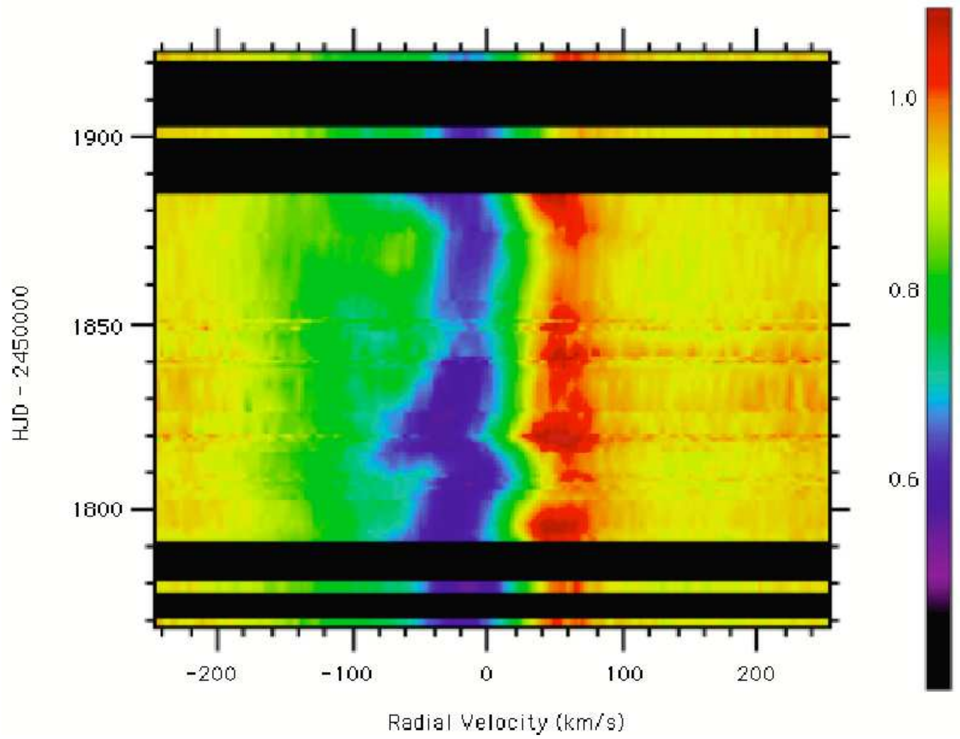

Fig. 4.— A dynamical spectrum of the Hα profile for the year 2000.

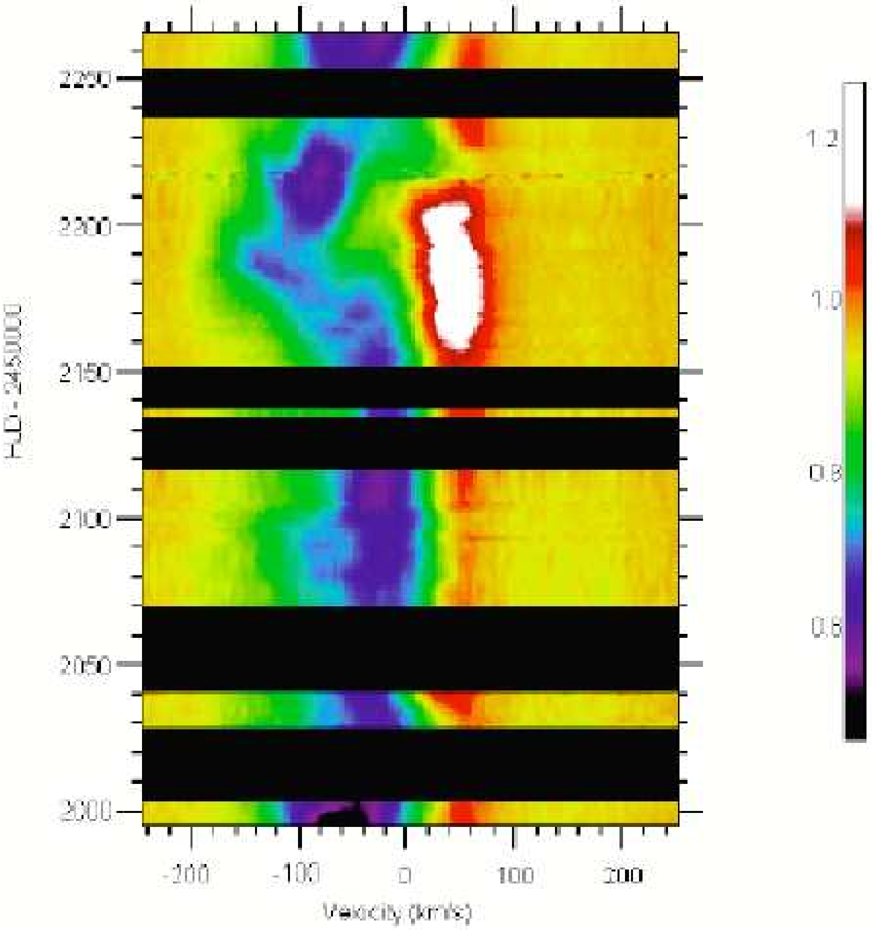

Fig. 5.— A dynamical spectrum of the Hα profile for the year 2001.

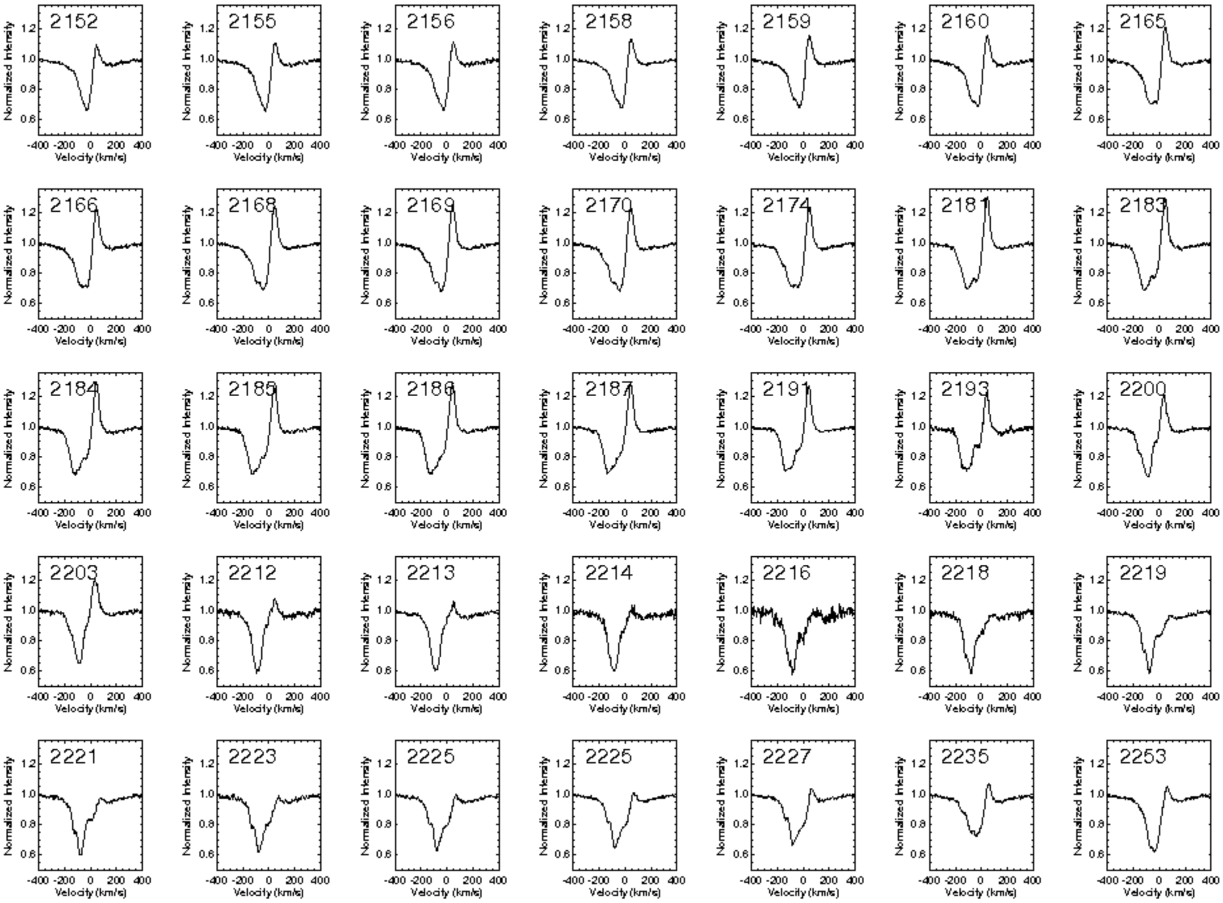

Fig. 6.— Line profiles of Hα observed during the major 2001 absorption and emission event. Features to note are the development of deep secondary and tertiary absorption components, the increase in the Hα emission and the near disappearence of the emission component beginning at HJD 2452214.5. All spectra are normalized to unity in the continuum and are plotted in the rest frame of Hα. The HJD - 2450000 is shown to the nearest integral day in each plot.

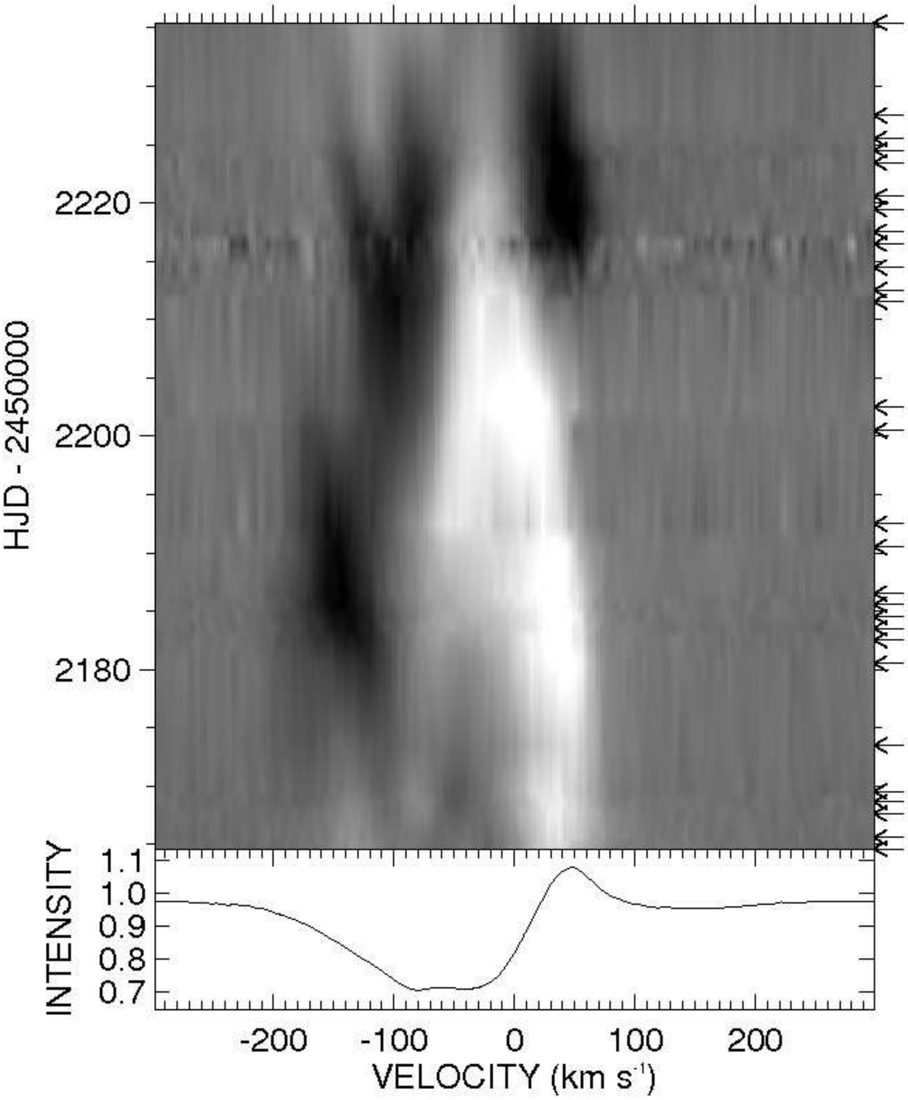

Fig. 7.— A dynamical spectrum of the Hα profile during the 2001 high velocity absorption event. The average profile for this time period, plotted in the lower panel, has been subtracted. There is an onset of high velocity absorption, followed by a second absorption event ∼ 40 days later. The second portion of this event is followed by an onset of absorption on the red wing, causing the emission to appear the weakest that we observed during the 5 years of data presented in this study.

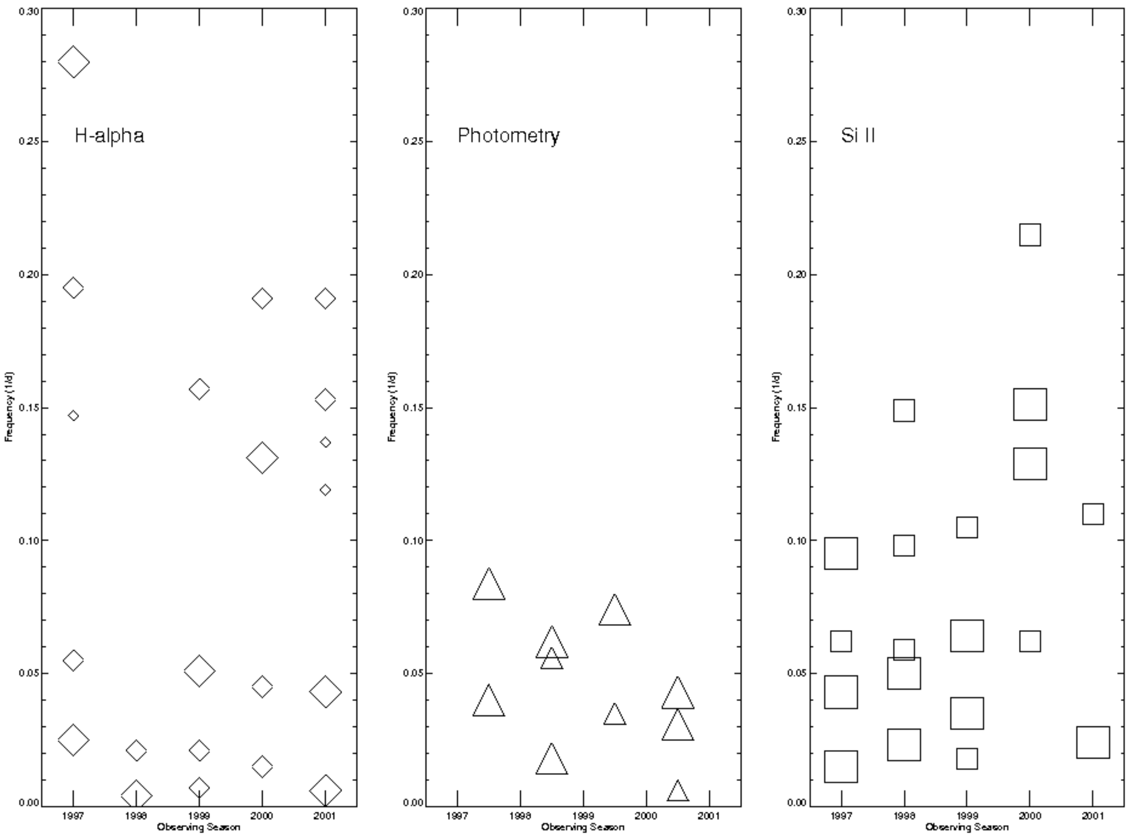

Fig. 8.— Plots of the frequencies derived in the CLEAN time series analysis. The symbol size is proportional to the relative strength of the derived frequency. The photometry produced similar results for all bandpasses, but only the *y* filter is plotted.

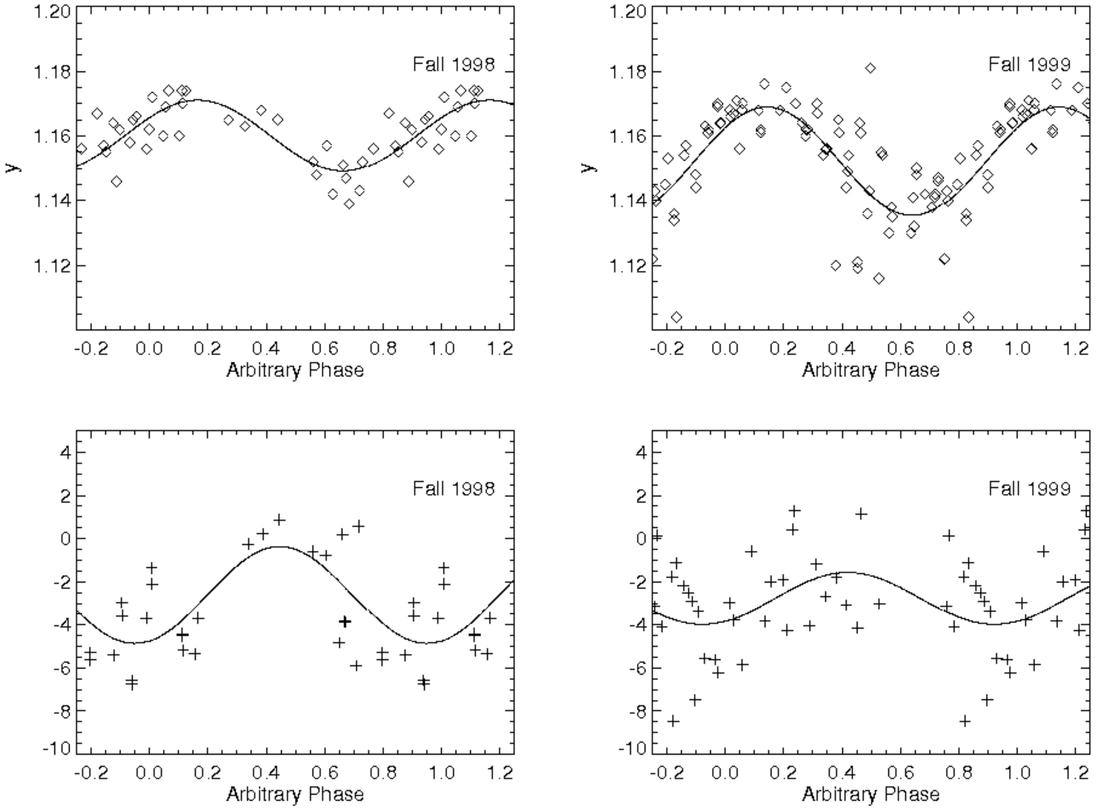

Fig. 9.— Plots of suspected radial pulsations seen in these data. On the top is the y band Strömgren photometry, and on the bottom are corresponding radial velocities. The periods are 17.8 days for the fall of 1998, and 13.4 days for the fall of 1999. Standard errors are less than 0.005 magnitudes for y, and about 1 km s^{-1} for the radial velocities. uvb magnitudes were also fitted, and the parameters of these fits are given in Table 4.

TABLE 1
Spectroscopic Measurements of the Hα profile and Si II doublet. This table can be found in its entirety online.

HJD	W_λ Hα, net (Å)	W_λ emission (Å)	W_λ absorption (Å)	V_r Si II 6347 (km s^{-1})	V_r Si II 6371 (km s^{-1})	$\sigma(V_r)$ (km s^{-1})
2450546.91051251	1.46	-0.29	1.75	-5.18	-4.88	0.81
2450588.86303180	1.24	-0.21	1.45	-1.50	-1.91	0.85
2450590.84395394	1.26	-0.21	1.48	-1.75	-1.57	0.77
2450591.85544913	1.28	-0.18	1.46	-1.73	-1.59	0.76
2450604.79591576	1.21	-0.20	1.42	-5.35	-4.69	1.00
2450609.87109713	1.26	-0.20	1.46	-4.20	-4.19	0.75
2450614.84276841	1.37	-0.22	1.59	-4.43	-4.53	0.76
2450623.77241360	1.13	-0.27	1.40	-2.05	-1.91	0.76
2450626.77451461	1.29	-0.22	1.51	-3.54	-4.14	0.96
2450627.73838157	1.21	-0.24	1.44	-4.84	-4.68	0.77
2450628.78655021	1.24	-0.24	1.48	-4.03	-3.83	0.78
2450631.77347052	1.33	-0.15	1.49	-2.55	-2.67	0.76
2450632.84827024	1.31	-0.16	1.46	-2.75	-3.12	0.84
2450635.85337284	1.45	-0.15	1.60	-3.05	-3.52	0.89
2450640.80576980	1.29	-0.18	1.46	-4.39	-4.66	0.80
2450643.76409389	1.20	-0.17	1.38	-6.35	-5.55	1.10
2450645.78557716	1.26	-0.17	1.44	-4.51	-4.55	0.75
2450649.89552412	1.20	-0.20	1.40	-5.32	-5.76	0.87
2450654.69862821	1.12	-0.28	1.39	-7.64	-6.88	1.07
2450660.74224343	1.23	-0.31	1.55	-4.07	-4.08	0.75
2450661.78846059	1.09	-0.29	1.38	-5.58	-5.43	0.76
2450663.72390025	1.13	-0.31	1.43	-5.50	-5.53	0.75
2450665.74104598	1.15	-0.29	1.44	-3.30	-3.11	0.77
2450666.73503305	1.16	-0.25	1.41	-2.14	-2.49	0.83
2450668.73985444	1.13	-0.26	1.39	-1.02	-1.58	0.94
2450669.69969583	0.84	-0.23	1.07	-0.86	-1.27	0.85
2450670.69620772	1.33	-0.23	1.56	-2.31	-2.93	0.97
2450674.64682815	1.32	-0.22	1.55	-7.20	-6.88	0.82

Table 1—*Continued*

HJD	W_λ Hα, net (Å)	W_λ emission (Å)	W_λ absorption (Å)	V_r Si II 6347 (km s^{-1})	V_r Si II 6371 (km s^{-1})	$\sigma(V_r)$ (km s^{-1})
2450684.61903913	1.24	-0.29	1.52	-4.31	-3.94	0.84
2450688.67315596	1.21	-0.21	1.41	-2.41	-2.60	0.77
2450689.70227578	1.22	-0.26	1.48	-2.58	-2.27	0.81
2450693.67658389	1.24	-0.23	1.47	-5.03	-4.10	1.19
2450695.72257290	1.20	-0.23	1.43	-5.77	-5.46	0.81
2450696.70105945	1.19	-0.15	1.33	-6.19	-5.45	1.05
2450704.69342104	1.15	-0.22	1.38	-1.93	-1.64	0.80
2450707.60930136	1.26	-0.20	1.46	-1.98	-1.96	0.75
2450709.72386113	1.22	-0.18	1.40	-3.41	-4.29	1.16
2450710.58845668	1.28	-0.18	1.46	-3.94	-3.76	0.77
2450712.61052209	1.26	-0.17	1.44	-4.31	-4.35	0.75
2450713.62311954	1.24	-0.23	1.47	-5.21	-4.18	1.27
2450715.60945511	1.26	-0.23	1.49	-4.15	-3.39	1.07
2450716.60215994	1.25	-0.22	1.47	-4.74	-3.66	1.31
2450717.57613373	1.26	-0.21	1.46	-4.43	-3.75	1.01
2450718.55766077	1.25	-0.20	1.45	-4.15	-3.72	0.86
2450719.57555580	1.22	-0.25	1.47	-4.06	-4.11	0.75
2450723.53224540	1.31	-0.28	1.58	-4.28	-4.50	0.78
2450724.50313663	1.35	-0.20	1.55	-4.60	-5.35	1.06
2450725.53217602	1.29	-0.22	1.51	-4.95	-5.29	0.82
2450727.59407425	1.27	-0.21	1.48	-5.04	-5.39	0.83
2450728.63555574	1.23	-0.20	1.42	-4.55	-4.93	0.84
2450729.52496529	1.15	-0.21	1.36	-4.67	-4.91	0.79
2450730.58291626	1.16	-0.21	1.37	-4.24	-4.15	0.76
2450731.64684010	1.09	-0.20	1.29	-3.84	-4.26	0.86
2450732.55339146	1.05	-0.21	1.26	-3.21	-3.22	0.75
2450736.53490734	1.08	-0.23	1.31	-2.14	-1.55	0.95
2450739.56125069	1.07	-0.21	1.27	-1.27	-1.70	0.86

TABLE 1—*Continued*

HJD	W_λ Hα, net (Å)	W_λ emission (Å)	W_λ absorption (Å)	V_r Si II 6347 (km s^{-1})	V_r Si II 6371 (km s^{-1})	$\sigma(V_r)$ (km s^{-1})
2450740.58932877	1.11	-0.20	1.31	-2.70	-2.27	0.86
2450741.53111076	1.12	-0.22	1.34	-1.65	-1.19	0.88
2450742.50016212	1.13	-0.24	1.36	-1.41	-1.19	0.78
2450743.50555947	1.18	-0.19	1.37	-0.97	-1.14	0.77
2450750.55849728	1.05	-0.23	1.28	-2.02	-0.97	1.29
2450752.56531801	1.11	-0.23	1.34	-0.18	0.79	1.23
2450762.49980709	1.18	-0.17	1.35	-1.51	-2.54	1.27
2450765.51684137	1.32	-0.13	1.45	-1.39	-1.35	0.75
2450770.47501183	1.26	-0.12	1.39	-4.05	-4.24	0.77
2450777.49181747	1.28	-0.14	1.42	-2.38	-2.73	0.83
2450798.47763920	1.50	-0.12	1.62	-2.33	-2.26	0.75
2450799.48850632	1.53	-0.10	1.63	-2.86	-2.39	0.89
2450800.52262673	1.50	-0.13	1.63	-3.62	-3.31	0.81
2450950.88095748	1.23	-0.46	1.90	-1.45	-1.20	0.79
2450955.85326243	1.44	-0.50	1.86	-1.42	-1.49	0.75
2450972.84059198	1.36	-0.33	1.95	-1.80	-2.02	0.78
2450999.77149517	1.62	-0.46	2.17	-4.09	-4.24	0.76
2451000.73309465	1.71	-0.52	2.06	-4.88	-4.72	0.77
2451004.79542603	1.54	-0.46	1.90	-4.98	-4.69	0.80
2451006.80721263	1.44	-0.36	1.73	-3.62	-3.51	0.76
2451021.75284438	1.37	-0.43	1.96	-4.83	-4.75	0.75
2451027.69932164	1.52	-0.38	1.88	-3.74	-3.69	0.75
2451028.69395310	1.50	-0.51	1.86	-4.17	-4.08	0.76
2451038.67103865	1.35	-0.36	1.73	-0.84	-0.47	0.84
2451044.79884184	1.37	-0.52	1.88	-7.21	-7.41	0.78
2451045.76414008	1.36	-0.47	1.88	-6.93	-6.24	1.02
2451051.67669180	1.41	-0.50	1.93	-2.44	-2.37	0.75
2451052.74531801	1.43	-0.44	1.96	-2.27	-2.05	0.78

Table 1—*Continued*

HJD	W_λ Hα, net (Å)	W_λ emission (Å)	W_λ absorption (Å)	V_r Si II 6347 (km s^{-1})	V_r Si II 6371 (km s^{-1})	$\sigma(V_r)$ (km s^{-1})
2451055.70155940	1.52	-0.48	2.00	-2.84	-2.84	0.75
2451057.67934585	1.52	-0.40	1.77	-4.38	-4.74	0.83
2451061.74683731	1.37	-0.37	1.76	-3.30	-2.73	0.94
2451062.70667893	1.39	-0.37	1.80	-2.94	-2.39	0.93
2451065.65878460	1.43	-0.41	1.84	-1.24	-0.97	0.80
2451066.63236443	1.43	-0.35	1.75	-3.71	-2.60	1.34
2451067.60498553	1.40	-0.42	1.78	-4.40	-3.89	0.91
2451068.71211093	1.36	-0.42	1.69	-5.04	-4.62	0.86
2451070.72930597	1.28	-0.33	1.66	-3.34	-2.85	0.90
2451075.53823459	1.33	-0.38	1.75	-2.91	-2.74	0.77
2451077.54643286	1.36	-0.36	1.68	-3.43	-2.99	0.87
2451079.57380094	1.32	-0.38	1.68	-4.92	-4.74	0.77
2451080.59926455	1.30	-0.46	1.75	-6.14	-5.66	0.89
2451083.61306955	1.29	-0.40	1.80	-5.77	-5.03	1.05
2451085.60670703	1.40	-0.45	1.83	-3.88	-3.48	0.85
2451088.57064794	1.38	-0.48	1.72	-5.33	-5.38	0.75
2451096.56685999	1.24	-0.48	1.70	-0.96	-0.59	0.84
2451097.55166005	1.22	-0.45	1.71	0.20	0.18	0.75
2451098.53583451	1.25	-0.38	1.68	0.56	0.62	0.75
2451102.52214259	1.30	-0.33	1.62	-6.81	-6.69	0.76
2451105.61378888	1.29	-0.38	1.67	-4.65	-4.35	0.81
2451106.58253566	1.29	-0.35	1.68	-4.06	-3.31	1.06
2451109.63728077	1.33	-0.35	1.68	-0.26	-0.25	0.75
2451110.50936285	1.33	-0.30	1.64	-0.11	0.56	1.01
2451111.50936280	1.34	-0.29	1.76	0.79	0.96	0.77
2451113.57118501	1.47	-0.29	1.80	-0.63	-0.57	0.75
2451115.51881552	1.51	-0.35	1.74	-3.71	-3.94	0.78
2451121.53755176	1.39	-0.46	1.50	-1.42	-1.28	0.76

Table 1—*Continued*

HJD	W_λ Hα, net (Å)	W_λ emission (Å)	W_λ absorption (Å)	V_r Si II 6347 (km s^{-1})	V_r Si II 6371 (km s^{-1})	$\sigma(V_r)$ (km s^{-1})
2451135.58661100	1.03	-0.42	1.30	-5.14	-5.46	0.82
2451137.51457740	0.88	-0.43	1.36	-3.11	-2.82	0.80
2451141.54538907	0.93	-0.48	1.43	-3.23	-2.81	0.86
2451144.47399910	0.96	-0.48	1.48	-2.05	-2.16	0.76
2451145.46913573	1.00	-0.38	1.39	-2.07	-1.61	0.88
2451146.48616081	1.01	-0.39	1.59	-1.63	-1.49	0.76
2451149.50689755	1.19	-0.30	1.59	-2.69	-2.54	0.76
2451157.49058970	1.29	-0.24	1.63	-1.07	-1.13	0.75
2451159.50352561	1.39	-0.17	1.63	1.09	0.69	0.85
2451160.50281023	1.46	-0.22	1.72	-0.59	-1.38	1.09
2451162.53478797	1.50	-0.19	1.69	-3.70	-3.90	0.78
2451163.47022251	1.50	-0.43	1.89	-4.44	-4.72	0.80
2451336.80563403	1.46	-0.45	1.85	-3.66	-4.00	0.82
2451338.84190551	1.40	-0.50	1.65	-5.16	-4.83	0.82
2451344.80036071	1.15	-0.39	1.52	-3.58	-3.29	0.80
2451348.85423465	1.13	-0.52	1.75	-3.19	-3.08	0.76
2451350.84189368	1.23	-0.40	1.83	-0.93	-0.73	0.78
2451355.82954285	1.43	-0.42	1.69	-4.61	-4.32	0.80
2451364.80753528	1.27	-0.54	1.84	-1.04	-0.93	0.76
2451365.84349881	1.30	-0.53	1.78	0.71	1.14	0.86
2451366.81577188	1.26	-0.41	1.72	-0.36	1.53	2.03
2451367.81323986	1.32	-0.37	1.90	1.75	3.84	2.22
2451369.87641275	1.53	-0.41	1.89	1.83	1.70	0.76
2451370.83326650	1.48	-0.33	1.93	4.54	4.39	0.76
2451371.86956697	1.61	-0.24	1.93	0.75	0.30	0.87
2451376.84562954	1.70	-0.24	1.94	-2.38	-2.76	0.84
2451390.79296231	1.69	-0.19	1.74	-3.51	-3.85	0.82
2451392.81798543	1.56	-0.31	2.02	-8.57	-8.63	0.75

Table 1—*Continued*

HJD	W_λ Hα, net (Å)	W_λ emission (Å)	W_λ absorption (Å)	V_r Si II 6347 (km s^{-1})	V_r Si II 6371 (km s^{-1})	$\sigma(V_r)$ (km s^{-1})
2451393.77638712	1.71	-0.42	1.60	-10.83	-10.12	1.03
2451399.79525191	1.18	-0.37	1.71	-5.80	-5.50	0.81
2451411.69902630	1.34	-0.43	1.67	-5.58	-4.93	0.99
2451419.73773457	1.24	-0.60	1.87	-6.22	-5.12	1.33
2451420.72246949	1.27	-0.36	1.53	-6.76	-5.23	1.70
2451421.64964821	1.17	-0.45	1.70	-5.87	-6.37	0.90
2451423.63147511	1.25	-0.52	1.78	-4.46	-4.50	0.75
2451424.65571363	1.27	-0.53	1.84	-4.99	-2.63	2.48
2451426.69744491	1.31	-0.44	1.73	-4.58	-4.45	0.76
2451435.62443607	1.29	-0.38	1.58	-4.82	-2.83	2.13
2451436.65566424	1.19	-0.43	1.60	-4.20	-4.28	0.75
2451437.67301701	1.17	-0.38	1.71	-3.85	-4.22	0.84
2451444.75422616	1.33	-0.28	1.58	-1.97	-1.58	0.85
2451445.67147021	1.30	-0.38	1.73	-2.80	-3.04	0.79
2451447.60288468	1.35	-0.42	1.65	-3.99	-3.54	0.87
2451457.69956882	1.24	-0.35	1.56	-3.94	-4.23	0.80
2451458.67892679	1.21	-0.36	1.58	-1.66	-2.71	1.29
2451459.67170132	1.22	-0.31	1.61	-5.60	-5.51	0.76
2451463.68991441	1.29	-0.32	1.79	0.23	0.61	0.84
2451466.66316974	1.46	-0.29	1.69	-3.91	-4.36	0.87
2451467.67782688	1.41	-0.25	1.73	-3.29	-2.77	0.91
2451471.61100990	1.48	-0.34	1.73	-8.61	-8.32	0.80
2451472.62301844	1.39	-0.40	1.81	-7.35	-7.63	0.80
2451473.53323194	1.41	-0.32	1.69	-5.85	-5.38	0.89
2451476.66490172	1.37	-0.46	1.88	-1.96	-1.88	0.75
2451478.61499964	1.42	-0.23	1.62	-2.69	-2.70	0.75
2451479.55320231	1.39	-0.46	1.64	-2.85	-3.32	0.89
2451487.60409752	1.18	-0.48	1.66	-3.22	-2.77	0.87

Table 1—*Continued*

HJD	W_λ Hα, net (Å)	W_λ emission (Å)	W_λ absorption (Å)	V_r Si II 6347 (km s^{-1})	V_r Si II 6371 (km s^{-1})	$\sigma(V_r)$ (km s^{-1})
2451488.59862064	1.17	-0.43	1.66	-0.67	-0.51	0.77
2451489.49557849	1.23	-0.39	1.70	-1.34	-2.64	1.50
2451490.57043052	1.32	-0.35	1.74	1.13	1.44	0.81
2451491.58998624	1.39	-0.34	1.74	-0.94	-1.46	0.91
2451492.51301154	1.40	-0.35	1.88	-1.67	-1.93	0.79
2451497.55375277	1.53	-0.26	1.79	-3.21	-3.06	0.76
2451498.55827275	1.53	-0.31	1.79	-1.19	-1.07	0.76
2451499.56391749	1.48	-0.31	1.73	-3.36	-3.39	0.75
2451500.48317052	1.42	-0.33	1.67	-6.33	-6.11	0.78
2451501.58749059	1.35	-0.38	1.84	-5.81	-5.91	0.76
2451512.50205306	1.46	-0.50	1.96	-2.49	-2.54	0.75
2451520.44426611	1.46	-0.45	1.93	1.25	1.05	0.78
2451524.45578348	1.47	-0.29	1.79	0.18	0.10	0.75
2451766.65352529	1.50	-0.30	1.99	-0.50	-0.59	0.76
2451777.69434071	1.69	-0.42	2.06	-1.64	-1.62	0.75
2451790.67409622	1.65	-0.44	1.85	-4.23	-3.86	0.84
2451792.64695412	1.41	-0.47	1.73	-4.75	-4.71	0.75
2451794.65323420	1.26	-0.37	1.74	-3.57	-3.03	0.92
2451800.64645313	1.37	-0.30	1.94	0.77	0.32	0.87
2451801.66190175	1.64	-0.33	1.83	-0.99	-1.18	0.77
2451803.70268037	1.50	-0.27	1.90	-2.21	-2.58	0.84
2451804.69867070	1.62	-0.35	2.07	0.49	0.12	0.84
2451805.66527417	1.73	-0.28	1.81	-2.03	-2.08	0.75
2451806.60222468	1.53	-0.25	1.82	-1.56	-1.85	0.80
2451807.66589659	1.57	-0.24	1.89	-1.66	-1.41	0.79
2451809.61068368	1.66	-0.35	2.06	-0.42	-0.46	0.75
2451812.58110413	1.71	-0.37	1.81	-6.04	-6.30	0.79
2451814.64967713	1.44	-0.40	1.84	-6.64	-6.02	0.97

Table 1—*Continued*

HJD	W_λ Hα, net (Å)	W_λ emission (Å)	W_λ absorption (Å)	V_r Si II 6347 (km s^{-1})	V_r Si II 6371 (km s^{-1})	$\sigma(V_r)$ (km s^{-1})
2451816.66153546	1.44	-0.50	1.65	-4.39	-3.72	1.01
2451817.70606781	1.15	-0.54	1.48	-1.74	-1.81	0.75
2451818.64572957	0.95	-0.38	1.69	9.14	8.26	1.16
2451819.56642114	1.31	-0.42	1.88	1.62	1.67	0.75
2451824.51645752	1.46	-0.43	1.68	-3.51	-3.64	0.76
2451825.49550015	1.26	-0.42	1.80	-4.03	-4.36	0.82
2451832.63255561	1.38	-0.29	1.55	-0.20	0.24	0.87
2451836.56151493	1.26	-0.31	1.88	-2.43	-1.63	1.10
2451837.56111674	1.56	-0.34	1.35	-1.34	-1.69	0.83
2451838.58314765	1.01	-0.28	1.37	-0.71	-1.07	0.83
2451839.49245117	1.09	-0.39	1.44	-1.88	-1.98	0.76
2451840.51696936	1.05	-0.20	1.77	-2.42	-3.43	1.26
2451845.50436195	1.56	-0.26	1.81	-5.35	-4.89	0.88
2451846.50508201	1.55	-0.34	1.46	-2.74	-2.37	0.84
2451847.64089982	1.12	-0.27	1.67	-3.02	-1.85	1.39
2451849.47802808	1.40	-0.28	1.81	-2.43	-1.64	1.09
2451853.47955711	1.53	-0.21	1.73	-0.11	-0.16	0.75
2451854.48402400	1.52	-0.32	1.84	-2.05	-2.00	0.75
2451864.47505721	1.53	-0.40	1.76	0.19	0.14	0.75
2451871.54475050	1.36	-0.31	1.64	-0.70	-0.56	0.76
2451873.50126078	1.33	-0.36	1.75	-2.86	-3.34	0.89
2451882.45217583	1.40	-0.22	1.61	-2.40	-1.89	0.91
2451901.47514821	1.38	-0.27	1.48	-1.65	-2.02	0.84
2451919.48566920	1.21	-0.18	1.87	-1.66	-1.55	0.76
2451994.89469939	1.69	-0.16	1.91	-2.82	-3.62	1.10
2451996.89223833	1.75	-0.14	1.86	2.06	1.85	0.78
2452001.97258815	1.71	-0.14	1.88	-1.79	-1.50	0.80
2452028.82093231	1.75	-0.14	1.54	-3.06	-2.88	0.77

Table 1—*Continued*

HJD	W_λ Hα, net (Å)	W_λ emission (Å)	W_λ absorption (Å)	V_r Si II 6347 (km s^{-1})	V_r Si II 6371 (km s^{-1})	$\sigma(V_r)$ (km s^{-1})
2452029.80038531	1.40	-0.12	1.52	-6.37	-6.04	0.82
2452033.78390954	1.41	-0.20	1.61	-1.19	-0.82	0.84
2452038.74861894	1.34	-0.22	1.56	-0.55	-1.33	1.08
2452039.81000001	1.23	-0.11	1.34	-2.68	-2.92	0.79
2452069.86191237	1.55	-0.11	1.66	-3.95	-3.26	1.02
2452074.87611819	1.47	-0.06	1.53	-3.61	-3.87	0.79
2452079.73171166	1.70	-0.08	1.78	-2.61	-2.40	0.78
2452086.86035902	1.64	-0.06	1.69	-2.14	-2.33	0.77
2452090.78253705	1.64	-0.09	1.73	-0.38	-0.35	0.75
2452092.78033792	1.44	-0.06	1.50	0.51	0.47	0.75
2452095.77715713	1.64	-0.07	1.70	-1.46	-1.72	0.79
2452096.80859715	1.60	-0.06	1.66	-6.28	-6.60	0.82
2452101.71120681	1.66	-0.11	1.77	-4.96	-4.84	0.76
2452102.75962414	1.41	-0.12	1.53	0.00	0.71	1.03
2452104.84014659	1.34	-0.11	1.45	1.51	2.93	1.61
2452105.75722569	1.41	-0.12	1.53	-3.72	-3.94	0.78
2452115.71436255	1.19	-0.14	1.32	-0.58	-0.48	0.76
2452151.66575579	1.09	-0.16	1.25	-2.73	-2.69	0.75
2452154.77190308	1.12	-0.21	1.32	-3.12	-2.40	1.04
2452155.75065970	1.09	-0.19	1.28	-1.98	-1.75	0.78
2452157.66480292	1.04	-0.24	1.27	-3.81	-3.50	0.81
2452158.63577953	1.02	-0.24	1.26	-0.75	-0.32	0.86
2452159.60004226	1.09	-0.26	1.35	-3.21	-2.82	0.85
2452163.66854221	1.11	-0.36	1.47	-5.43	-4.88	0.93
2452164.64596066	1.04	-0.36	1.40	-6.06	-5.55	0.91
2452165.59930458	1.00	-0.38	1.38	-5.42	-5.01	0.85
2452167.65179817	0.97	-0.43	1.41	-3.87	-2.95	1.19
2452168.64343776	1.01	-0.41	1.42	-2.93	-2.33	0.96

Table 1—*Continued*

HJD	W_λ Hα, net (Å)	W_λ emission (Å)	W_λ absorption (Å)	V_r Si II 6347 (km s^{-1})	V_r Si II 6371 (km s^{-1})	$\sigma(V_r)$ (km s^{-1})
2452169.54733498	1.05	-0.41	1.47	-2.43	-2.24	0.77
2452173.51536406	1.08	-0.38	1.47	-4.88	-4.71	0.77
2452180.52505513	0.96	-0.47	1.43	-1.10	-0.33	1.07
2452182.53683153	0.99	-0.50	1.49	-0.44	-0.12	0.82
2452183.55028786	1.01	-0.43	1.45	-6.20	-6.58	0.84
2452184.52438114	1.00	-0.46	1.46	-2.71	-2.17	0.92
2452185.57601779	0.97	-0.44	1.41	-3.36	-2.98	0.84
2452186.52787653	0.92	-0.50	1.42	-3.26	-2.94	0.82
2452190.51306572	0.85	-0.41	1.26	0.12	-0.13	0.79
2452192.50230576	0.93	-0.36	1.29	-0.88	-1.09	0.78
2452200.49032799	0.87	-0.36	1.23	-4.86	-4.65	0.78
2452202.51007565	0.75	-0.43	1.18	-3.96	-3.18	1.08
2452211.54627200	1.18	-0.21	1.39	1.94	1.19	1.06
2452212.53254794	1.28	-0.14	1.42	2.05	1.65	0.85
2452214.46641976	1.39	-0.11	1.50	2.06	1.35	1.03
2452216.49511221	1.44	-0.17	1.61	1.10	0.04	1.30
2452217.53935808	1.54	-0.05	1.59	-0.05	-1.15	1.33
2452218.46923395	1.47	-0.05	1.52	0.16	0.41	0.79
2452219.47158286	1.50	-0.03	1.53	0.09	0.05	0.75
2452220.54794420	1.48	-0.05	1.53	-0.36	-0.13	0.78
2452223.46755044	1.49	-0.05	1.54	-2.24	-1.95	0.80
2452224.50767394	1.46	-0.07	1.53	-2.59	-2.19	0.85
2452225.48495306	1.38	-0.07	1.46	-2.30	-2.47	0.77
2452227.49988936	1.28	-0.10	1.38	-1.97	-1.86	0.76
2452235.45532754	1.20	-0.14	1.35	0.40	0.75	0.83
2452253.46989869	1.37	-0.13	1.50	-3.33	-2.82	0.91
2452262.46741699	1.51	-0.10	1.61	1.70	2.14	0.87
2452264.49168601	1.53	-0.09	1.62	2.76	3.34	0.95

TABLE 1—*Continued*

HJD	W_λ Hα, net (Å)	W_λ emission (Å)	W_λ absorption (Å)	V_r Si II 6347 (km s^{-1})	V_r Si II 6371 (km s^{-1})	$\sigma(V_r)$ (km s^{-1})
2452265.50806281	1.61	-0.07	1.69	4.11	4.31	0.78

Table 2

Strömgren Photometry of Deneb. This table can be found in its entirety online.

HJD	u	v	b	y	$u-b$	$b-y$	c_1	m_1
2450750.6404	2.229	1.347	1.172	1.171	1.057	0.001	0.707	0.174
2450751.6399	2.222	1.336	1.164	1.158	1.058	0.006	0.714	0.166
2450752.6566	2.215	1.332	1.158	1.153	1.057	0.005	0.709	0.169
2450753.6364	2.210	1.322	1.155	1.141	1.055	0.014	0.721	0.153
2450754.6564	2.197	1.314	1.142	1.142	1.055	0.000	0.711	0.172
2450756.6545	2.174	1.299	1.124	1.121	1.050	0.003	0.700	0.172
2450757.6456	2.178	1.295	1.122	1.119	1.056	0.003	0.710	0.170
2450760.6463	2.181	1.312	1.134	1.128	1.047	0.006	0.691	0.172
2450767.6317	2.186	1.305	1.133	1.128	1.053	0.005	0.709	0.167
2450768.6054	2.182	1.297	1.123	1.124	1.059	-0.001	0.711	0.175
2450769.6084	2.175	1.292	1.121	1.121	1.054	0.000	0.712	0.171
2450771.6043	2.187	1.306	1.129	1.128	1.058	0.001	0.704	0.176
2450772.5904	2.176	1.288	1.118	1.112	1.058	0.006	0.718	0.164
2450781.5898	2.164	1.285	1.109	1.109	1.055	0.000	0.703	0.176
2450782.5898	2.166	1.284	1.108	1.104	1.058	0.004	0.706	0.172
2450792.5734	2.197	1.301	1.134	1.132	1.063	0.002	0.729	0.165
2450793.5734	2.184	1.306	1.133	1.121	1.051	0.012	0.705	0.161
2450919.9904	2.203	1.329	1.147	1.145	1.056	0.002	0.692	0.180
2450920.9905	2.209	1.333	1.148	1.148	1.061	0.000	0.691	0.185
2450921.9873	2.209	1.340	1.156	1.154	1.053	0.002	0.685	0.182
2450922.9855	2.203	1.423	1.155	1.154	1.048	0.001	0.512	0.267
2450926.9763	2.191	1.322	1.140	1.137	1.051	0.003	0.687	0.179
2450928.9701	2.181	1.301	1.132	1.124	1.049	0.008	0.711	0.161
2450931.9586	2.186	1.311	1.128	1.130	1.058	-0.002	0.692	0.185
2450932.9547	2.182	1.315	1.137	1.134	1.045	0.003	0.689	0.175
2450933.9526	2.192	1.318	1.139	1.134	1.053	0.005	0.695	0.174
2450934.9499	2.195	1.328	1.147	1.139	1.048	0.008	0.686	0.173
2450936.9446	2.196	1.322	1.141	1.141	1.055	0.000	0.693	0.181
2450938.9448	2.195	1.317	1.139	1.139	1.056	0.000	0.700	0.178
2450940.9372	2.226	1.338	1.163	1.156	1.063	0.007	0.713	0.168

Table 2—*Continued*

HJD	u	v	b	y	$u-b$	$b-y$	c_1	m_1
2450942.9296	2.223	1.351	1.166	1.162	1.057	0.004	0.687	0.181
2450943.9234	2.217	1.347	1.167	1.163	1.050	0.004	0.690	0.176
2450944.9278	2.207	1.344	1.175	1.151	1.032	0.024	0.694	0.145
2450946.9188	2.201	1.322	1.145	1.140	1.056	0.005	0.702	0.172
2450948.9128	2.200	1.335	1.152	1.142	1.048	0.010	0.682	0.173
2450949.9104	2.203	1.336	1.153	1.146	1.050	0.007	0.684	0.176
2450951.9033	2.208	1.345	1.164	1.163	1.044	0.001	0.682	0.180
2450957.8895	2.206	1.342	1.159	1.155	1.047	0.004	0.681	0.179
2450959.8865	2.195	1.329	1.145	1.142	1.050	0.003	0.682	0.181
2450960.8905	2.185	1.329	1.126	1.127	1.059	-0.001	0.653	0.204
2450961.8762	2.180	1.320	1.138	1.132	1.042	0.006	0.678	0.176
2450962.8976	2.179	1.309	1.133	1.126	1.046	0.007	0.694	0.169
2450965.8725	2.199	1.317	1.135	1.135	1.064	0.000	0.700	0.182
2450966.8626	2.201	1.315	1.141	1.140	1.060	0.001	0.712	0.173
2450966.8776	2.210	1.314	1.138	1.140	1.072	-0.002	0.720	0.178
2450968.8595	2.230	1.340	1.160	1.155	1.070	0.005	0.710	0.175
2450968.8668	2.230	1.337	1.158	1.150	1.072	0.008	0.714	0.171
2450969.8564	2.237	1.346	1.169	1.161	1.068	0.008	0.714	0.169
2450969.9585	2.239	1.336	1.163	1.161	1.076	0.002	0.730	0.171
2450970.8536	2.242	1.359	1.175	1.167	1.067	0.008	0.699	0.176
2450970.8604	2.241	1.353	1.172	1.168	1.069	0.004	0.707	0.177
2450972.8473	2.233	1.340	1.161	1.155	1.072	0.006	0.714	0.173
2450972.8626	2.229	1.343	1.161	1.157	1.068	0.004	0.704	0.178
2450973.8455	2.202	1.319	1.181	1.169	1.021	0.012	0.745	0.126
2450974.8404	2.193	1.314	1.134	1.133	1.059	0.001	0.699	0.179
2450977.8316	2.187	1.317	1.146	1.142	1.041	0.004	0.699	0.167
2450977.8396	2.197	1.334	1.149	1.140	1.048	0.009	0.678	0.176
2450977.8466	2.190	1.315	1.135	1.138	1.055	-0.003	0.695	0.183
2450977.8545	2.201	1.327	1.146	1.142	1.055	0.004	0.693	0.177
2450977.8612	2.192	1.326	1.143	1.142	1.049	0.001	0.683	0.182

TABLE 2—*Continued*

HJD	u	v	b	y	$u-b$	$b-y$	c_1	m_1
2450977.8694	2.192	1.331	1.145	1.140	1.047	0.005	0.675	0.181
2450977.8764	2.179	1.320	1.144	1.144	1.035	0.000	0.683	0.176
2450977.8843	2.187	1.325	1.141	1.141	1.046	0.000	0.678	0.184
2450977.8909	2.189	1.321	1.150	1.143	1.039	0.007	0.697	0.164
2450977.8993	2.190	1.328	1.143	1.143	1.047	0.000	0.677	0.185
2450977.9063	2.182	1.321	1.138	1.141	1.044	-0.003	0.678	0.186
2450977.9140	2.183	1.327	1.147	1.140	1.036	0.007	0.676	0.173
2450977.9204	2.192	1.322	1.140	1.142	1.052	-0.002	0.688	0.184
2450977.9289	2.191	1.326	1.143	1.138	1.048	0.005	0.682	0.178
2450977.9366	2.188	1.320	1.143	1.141	1.045	0.002	0.691	0.175
2450977.9436	2.191	1.325	1.145	1.138	1.046	0.007	0.686	0.173
2450977.9505	2.188	1.319	1.143	1.140	1.045	0.003	0.693	0.173
2450978.8370	2.187	1.323	1.143	1.142	1.044	0.001	0.684	0.179
2450978.8445	2.188	1.318	1.149	1.145	1.039	0.004	0.701	0.165
2450978.8516	2.194	1.329	1.149	1.144	1.045	0.005	0.685	0.175
2450978.8596	2.189	1.327	1.149	1.143	1.040	0.006	0.684	0.172
2450978.8666	2.193	1.316	1.147	1.142	1.046	0.005	0.708	0.164
2450978.8745	2.190	1.320	1.150	1.141	1.040	0.009	0.700	0.161
2450978.8812	2.195	1.324	1.148	1.143	1.047	0.005	0.695	0.171
2450978.8894	2.194	1.318	1.148	1.142	1.046	0.006	0.706	0.164
2450978.8964	2.189	1.320	1.146	1.142	1.043	0.004	0.695	0.170
2450978.9043	2.195	1.323	1.147	1.145	1.048	0.002	0.696	0.174
2450978.9103	2.189	1.321	1.144	1.143	1.045	0.001	0.691	0.176
2450978.9193	2.193	1.325	1.145	1.142	1.048	0.003	0.688	0.177
2450978.9263	2.193	1.324	1.145	1.141	1.048	0.004	0.690	0.175
2450978.9342	2.194	1.322	1.147	1.143	1.047	0.004	0.697	0.171
2450978.9405	2.196	1.327	1.146	1.145	1.050	0.001	0.688	0.180
2450978.9489	2.197	1.333	1.146	1.144	1.051	0.002	0.677	0.185
2450978.9566	2.196	1.330	1.148	1.144	1.048	0.004	0.684	0.178
2450979.8275	2.191	1.319	1.142	1.144	1.049	-0.002	0.695	0.179

Table 2—*Continued*

HJD	u	v	b	y	$u-b$	$b-y$	c_1	m_1
2450979.8348	2.194	1.321	1.148	1.143	1.046	0.005	0.700	0.168
2450979.8425	2.195	1.324	1.144	1.144	1.051	0.000	0.691	0.180
2450979.8497	2.200	1.326	1.147	1.142	1.053	0.005	0.695	0.174
2450979.8574	2.198	1.322	1.144	1.142	1.054	0.002	0.698	0.176
2450979.8646	2.201	1.321	1.147	1.144	1.054	0.003	0.706	0.171
2450979.8701	2.186	1.322	1.142	1.136	1.044	0.006	0.684	0.174
2450979.8786	2.196	1.321	1.148	1.142	1.048	0.006	0.702	0.167
2450979.8866	2.198	1.319	1.147	1.143	1.051	0.004	0.707	0.168
2450979.8938	2.195	1.315	1.151	1.143	1.044	0.008	0.716	0.156
2450979.9004	2.196	1.330	1.145	1.145	1.051	0.000	0.681	0.185
2450979.9086	2.196	1.323	1.145	1.141	1.051	0.004	0.695	0.174
2450979.9143	2.189	1.316	1.141	1.138	1.048	0.003	0.698	0.172
2450979.9209	2.197	1.323	1.146	1.143	1.051	0.003	0.697	0.174
2450979.9292	2.197	1.328	1.145	1.141	1.052	0.004	0.686	0.179
2450979.9365	2.197	1.323	1.146	1.144	1.051	0.002	0.697	0.175
2450979.9439	2.198	1.324	1.147	1.145	1.051	0.002	0.697	0.175
2450980.8304	2.197	1.326	1.148	1.144	1.049	0.004	0.693	0.174
2450980.8389	2.201	1.326	1.148	1.149	1.053	-0.001	0.697	0.179
2450982.8244	2.212	1.330	1.155	1.146	1.057	0.009	0.707	0.166
2450983.8176	2.205	1.339	1.154	1.139	1.051	0.015	0.681	0.170
2450983.9336	2.214	1.339	1.157	1.152	1.057	0.005	0.693	0.177
2450984.8142	2.204	1.346	1.157	1.156	1.047	0.001	0.669	0.188
2450984.8205	2.210	1.347	1.159	1.157	1.051	0.002	0.675	0.186
2450985.8176	2.206	1.345	1.161	1.154	1.045	0.007	0.677	0.177
2450985.8255	2.210	1.349	1.167	1.160	1.043	0.007	0.679	0.175
2450985.8328	2.208	1.353	1.163	1.157	1.045	0.006	0.665	0.184
2450985.8405	2.212	1.355	1.164	1.156	1.048	0.008	0.666	0.183
2450985.8476	2.217	1.348	1.160	1.163	1.057	-0.003	0.681	0.191
2450985.8555	2.208	1.353	1.161	1.156	1.047	0.005	0.663	0.187
2450985.8625	2.214	1.345	1.165	1.156	1.049	0.009	0.689	0.171

TABLE 2—*Continued*

HJD	u	v	b	y	$u-b$	$b-y$	c_1	m_1
2450985.8703	2.213	1.349	1.165	1.157	1.048	0.008	0.680	0.176
2450985.8776	2.209	1.350	1.161	1.156	1.048	0.005	0.670	0.184
2450985.8852	2.210	1.346	1.158	1.154	1.052	0.004	0.676	0.184
2450985.8925	2.214	1.347	1.163	1.155	1.051	0.008	0.683	0.176
2450985.9003	2.204	1.340	1.164	1.154	1.040	0.010	0.688	0.166
2450985.9075	2.209	1.352	1.157	1.155	1.052	0.002	0.662	0.193
2450985.9149	2.212	1.349	1.162	1.154	1.050	0.008	0.676	0.179
2450985.9224	2.215	1.343	1.160	1.154	1.055	0.006	0.689	0.177
2450985.9296	2.211	1.343	1.163	1.157	1.048	0.006	0.688	0.174
2450985.9375	2.215	1.354	1.160	1.160	1.055	0.000	0.667	0.194
2450985.9448	2.209	1.343	1.161	1.159	1.048	0.002	0.684	0.180
2450985.9524	2.212	1.343	1.160	1.157	1.052	0.003	0.686	0.180
2450985.9596	2.212	1.343	1.165	1.156	1.047	0.009	0.691	0.169
2450985.9673	2.211	1.348	1.161	1.154	1.050	0.007	0.676	0.180
2450986.8146	2.205	1.341	1.159	1.165	1.046	-0.006	0.682	0.188
2450986.8903	2.210	1.338	1.158	1.154	1.052	0.004	0.692	0.176
2450987.8073	2.214	1.346	1.159	1.151	1.055	0.008	0.681	0.179
2450988.8035	2.206	1.333	1.152	1.144	1.054	0.008	0.692	0.173
2450988.8825	2.212	1.340	1.153	1.146	1.059	0.007	0.685	0.180
2450989.8029	2.203	1.333	1.148	1.149	1.055	-0.001	0.685	0.186
2450990.8066	2.199	1.349	1.153	1.146	1.046	0.007	0.654	0.189
2450990.8864	2.206	1.339	1.153	1.145	1.053	0.008	0.681	0.178
2450991.7985	2.201	1.343	1.156	1.143	1.045	0.013	0.671	0.174
2450991.8876	2.207	1.343	1.154	1.147	1.053	0.007	0.675	0.182
2450992.7955	2.193	1.344	1.161	1.155	1.032	0.006	0.666	0.177
2450993.7905	2.207	1.346	1.157	1.154	1.050	0.003	0.672	0.186
2450994.7875	2.194	1.340	1.150	1.149	1.044	0.001	0.664	0.189
2450994.9665	2.202	1.333	1.155	1.148	1.047	0.007	0.691	0.171
2450995.8553	2.199	1.325	1.146	1.145	1.053	0.001	0.695	0.178
2450996.9302	2.195	1.316	1.149	1.140	1.046	0.009	0.712	0.158

TABLE 2—*Continued*

HJD	u	v	b	y	$u-b$	$b-y$	c_1	m_1
2451081.6695	2.202	1.324	1.159	1.156	1.043	0.003	0.713	0.162
2451082.6023	2.212	1.337	1.166	1.167	1.046	-0.001	0.704	0.172
2451083.6003	2.211	1.340	1.165	1.164	1.046	0.001	0.696	0.174
2451084.6002	2.211	1.334	1.162	1.158	1.049	0.004	0.705	0.168
2451085.6203	2.211	1.337	1.163	1.156	1.048	0.007	0.700	0.167
2451086.6404	2.214	1.325	1.159	1.160	1.055	-0.001	0.723	0.167
2451087.6235	2.214	1.331	1.157	1.160	1.057	-0.003	0.709	0.177
2451090.6225	2.213	1.334	1.167	1.165	1.046	0.002	0.712	0.165
2451091.6253	2.212	1.338	1.164	1.163	1.048	0.001	0.700	0.173
2451092.6186	2.208	1.346	1.170	1.168	1.038	0.002	0.686	0.174
2451093.6176	2.217	1.347	1.169	1.165	1.048	0.004	0.692	0.174
2451096.6155	2.194	1.332	1.161	1.157	1.033	0.004	0.691	0.167
2451097.6146	2.185	1.321	1.154	1.151	1.031	0.003	0.697	0.164
2451098.6035	2.183	1.319	1.146	1.143	1.037	0.003	0.691	0.170
2451101.6001	2.206	1.323	1.154	1.146	1.052	0.008	0.714	0.161
2451102.5998	2.217	1.336	1.163	1.165	1.054	-0.002	0.708	0.175
2451103.5885	2.215	1.333	1.168	1.162	1.047	0.006	0.717	0.159
2451104.5883	2.224	1.343	1.179	1.169	1.045	0.010	0.717	0.154
2451105.5875	2.237	1.346	1.183	1.174	1.054	0.009	0.728	0.154
2451105.6244	2.230	1.358	1.176	1.170	1.054	0.006	0.690	0.176
2451113.5905	2.188	1.334	1.130	1.152	1.058	-0.022	0.650	0.226
2451115.5894	2.194	1.320	1.149	1.147	1.045	0.002	0.703	0.169
2451116.5905	2.199	1.338	1.158	1.152	1.041	0.006	0.681	0.174
2451118.5911	2.201	1.331	1.159	1.157	1.042	0.002	0.698	0.170
2451119.5885	2.210	1.348	1.166	1.162	1.044	0.004	0.680	0.178
2451120.5902	2.213	1.340	1.168	1.166	1.045	0.002	0.701	0.170
2451121.5694	2.224	1.351	1.176	1.172	1.048	0.004	0.698	0.171
2451122.5690	2.225	1.354	1.176	1.174	1.049	0.002	0.693	0.176
2451123.6403	2.218	1.346	1.175	1.174	1.043	0.001	0.701	0.170
2451131.5902	2.195	1.314	1.150	1.148	1.045	0.002	0.717	0.162

Table 2—*Continued*

HJD	u	v	b	y	$u-b$	$b-y$	c_1	m_1
2451132.5875	2.196	1.313	1.147	1.142	1.049	0.005	0.717	0.161
2451133.5875	2.193	1.316	1.144	1.139	1.049	0.005	0.705	0.167
2451136.5709	2.197	1.329	1.163	1.155	1.034	0.008	0.702	0.158
2451290.9885	2.244	1.374	1.198	1.188	1.046	0.010	0.694	0.166
2451295.9834	2.221	1.364	1.186	1.180	1.035	0.006	0.679	0.172
2451298.9703	2.214	1.354	1.179	1.174	1.035	0.005	0.685	0.170
2451299.9647	2.214	1.349	1.177	1.173	1.037	0.004	0.693	0.168
2451300.9609	2.213	1.347	1.175	1.172	1.038	0.003	0.694	0.169
2451302.9603	2.234	1.349	1.175	1.183	1.059	-0.008	0.711	0.182
2451303.9644	2.242	1.354	1.182	1.182	1.060	0.000	0.716	0.172
2451304.9593	2.231	1.346	1.174	1.172	1.057	0.002	0.713	0.170
2451306.9786	2.225	1.335	1.168	1.169	1.057	-0.001	0.723	0.168
2451308.9736	2.208	1.339	1.163	1.165	1.045	-0.002	0.693	0.178
2451310.9669	2.196	1.324	1.149	1.150	1.047	-0.001	0.697	0.176
2451312.9293	2.193	1.324	1.150	1.146	1.043	0.004	0.695	0.170
2451313.9683	2.192	1.329	1.153	1.150	1.039	0.003	0.687	0.173
2451314.9254	2.203	1.334	1.160	1.155	1.043	0.005	0.695	0.169
2451315.9213	2.197	1.322	1.154	1.154	1.043	0.000	0.707	0.168
2451317.9453	2.203	1.329	1.156	1.154	1.047	0.002	0.701	0.171
2451318.9275	2.204	1.331	1.155	1.154	1.049	0.001	0.697	0.175
2451319.9283	2.200	1.336	1.157	1.156	1.043	0.001	0.685	0.178
2451320.9249	2.193	1.334	1.158	1.153	1.035	0.005	0.683	0.171
2451321.9326	2.190	1.334	1.160	1.157	1.030	0.003	0.682	0.171
2451322.9175	2.191	1.338	1.156	1.155	1.035	0.001	0.671	0.181
2451323.9184	2.193	1.335	1.158	1.150	1.035	0.008	0.681	0.169
2451324.9273	2.192	1.330	1.156	1.157	1.036	-0.001	0.688	0.175
2451325.9233	2.196	1.337	1.159	1.162	1.037	-0.003	0.681	0.181
2451326.9074	2.197	1.338	1.158	1.154	1.039	0.004	0.679	0.176
2451447.7241	2.242	1.360	1.178	1.171	1.064	0.007	0.700	0.175
2451448.7296	2.241	1.363	1.175	1.168	1.066	0.007	0.690	0.181

TABLE 2—*Continued*

HJD	u	v	b	y	$u-b$	$b-y$	c_1	m_1
2451449.7205	2.231	1.356	1.174	1.168	1.057	0.006	0.693	0.176
2451450.7197	2.227	1.347	1.170	1.164	1.057	0.006	0.703	0.171
2451451.7045	2.219	1.344	1.154	1.154	1.065	0.000	0.685	0.190
2451452.7455	2.194	1.329	1.144	1.144	1.050	0.000	0.680	0.185
2451453.7328	2.185	1.317	1.138	1.136	1.047	0.002	0.689	0.177
2451454.7100	2.177	1.310	1.131	1.130	1.046	0.001	0.688	0.178
2451455.7241	2.180	1.314	1.134	1.130	1.046	0.004	0.686	0.176
2451456.6853	2.187	1.330	1.144	1.138	1.043	0.006	0.671	0.180
2451458.7142	2.218	1.342	1.159	1.154	1.059	0.005	0.693	0.178
2451459.6947	2.224	1.350	1.168	1.163	1.056	0.005	0.692	0.177
2451465.6754	2.167	1.304	1.125	1.120	1.042	0.005	0.684	0.174
2451466.6700	2.169	1.303	1.121	1.121	1.048	0.000	0.684	0.182
2451466.6785	2.169	1.303	1.120	1.119	1.049	0.001	0.683	0.182
2451467.6596	2.169	1.299	1.115	1.116	1.054	-0.001	0.686	0.185
2451467.6671	2.168	1.300	1.117	1.116	1.051	0.001	0.685	0.182
2451470.6645	2.175	1.301	1.127	1.122	1.048	0.005	0.700	0.169
2451470.6801	2.176	1.302	1.127	1.122	1.049	0.005	0.699	0.170
2451471.6534	2.186	1.318	1.139	1.136	1.047	0.003	0.689	0.176
2451471.6601	2.192	1.321	1.138	1.134	1.054	0.004	0.688	0.179
2451472.6501	2.201	1.324	1.148	1.148	1.053	0.000	0.701	0.176
2451472.6584	2.201	1.326	1.147	1.144	1.054	0.003	0.696	0.176
2451473.6546	2.216	1.330	1.155	1.169	1.061	-0.014	0.711	0.189
2451473.6601	2.218	1.331	1.157	1.170	1.061	-0.013	0.713	0.187
2451474.6496	2.218	1.340	1.160	1.156	1.058	0.004	0.698	0.176
2451474.6571	2.219	1.340	1.162	1.156	1.057	0.006	0.701	0.172
2451475.6285	2.226	1.345	1.162	1.161	1.064	0.001	0.698	0.182
2451475.6361	2.220	1.346	1.168	1.162	1.052	0.006	0.696	0.172
2451477.6890	2.221	1.345	1.168	1.160	1.053	0.008	0.699	0.169
2451477.6974	2.221	1.342	1.168	1.162	1.053	0.006	0.705	0.168
2451478.6262	2.215	1.335	1.160	1.156	1.055	0.004	0.705	0.171

TABLE 2—*Continued*

HJD	u	v	b	y	$u-b$	$b-y$	c_1	m_1
2451478.6670	2.217	1.341	1.160	1.156	1.057	0.004	0.695	0.177
2451479.6305	2.206	1.330	1.155	1.149	1.051	0.006	0.701	0.169
2451479.6656	2.210	1.335	1.151	1.154	1.059	-0.003	0.691	0.187
2451480.6300	2.203	1.339	1.152	1.143	1.051	0.009	0.677	0.178
2451480.6700	2.177	1.317	1.141	1.181	1.036	-0.040	0.684	0.216
2451481.6254	2.197	1.325	1.142	1.138	1.055	0.004	0.689	0.179
2451481.6664	2.195	1.319	1.146	1.135	1.049	0.011	0.703	0.162
2451482.6301	2.190	1.323	1.144	1.141	1.046	0.003	0.688	0.176
2451482.6700	2.195	1.328	1.140	1.132	1.055	0.008	0.679	0.180
2451483.6185	2.187	1.323	1.146	1.141	1.041	0.005	0.687	0.172
2451483.6595	2.188	1.326	1.145	1.142	1.043	0.003	0.681	0.178
2451484.6565	2.196	1.333	1.150	1.145	1.046	0.005	0.680	0.178
2451485.6060	2.211	1.337	1.162	1.157	1.049	0.005	0.699	0.170
2451486.6090	2.216	1.350	1.167	1.161	1.049	0.006	0.683	0.177
2451486.6435	2.213	1.352	1.169	1.162	1.044	0.007	0.678	0.176
2451487.6077	2.219	1.355	1.171	1.168	1.048	0.003	0.680	0.181
2451487.6486	2.217	1.355	1.172	1.166	1.045	0.006	0.679	0.177
2451491.6033	2.240	1.354	1.173	1.170	1.067	0.003	0.705	0.178
2451491.6371	2.239	1.355	1.172	1.167	1.067	0.005	0.701	0.178
2451490.6306	2.239	1.359	1.173	1.170	1.066	0.003	0.694	0.183
2451492.5950	2.230	1.352	1.167	1.165	1.063	0.002	0.693	0.183
2451492.6351	2.232	1.353	1.172	1.161	1.060	0.011	0.698	0.170
2451493.5753	2.219	1.353	1.167	1.164	1.052	0.003	0.680	0.183
2451493.6274	2.225	1.349	1.164	1.161	1.061	0.003	0.691	0.182
2451494.5721	2.209	1.344	1.160	1.155	1.049	0.005	0.681	0.179
2451494.6242	2.208	1.344	1.161	1.154	1.047	0.007	0.681	0.176
2451496.5732	2.204	1.331	1.140	1.142	1.064	-0.002	0.682	0.193
2451497.5650	2.205	1.326	1.141	1.143	1.064	-0.002	0.694	0.187
2451497.6161	2.197	1.326	1.141	1.140	1.056	0.001	0.686	0.184
2451498.5655	2.208	1.331	1.145	1.104	1.063	0.041	0.691	0.145

TABLE 2—*Continued*

HJD	u	v	b	y	$u-b$	$b-y$	c_1	m_1
2451500.5725	2.230	1.336	1.163	1.164	1.067	-0.001	0.721	0.174
2451500.6043	2.226	1.341	1.166	1.164	1.060	0.002	0.710	0.173
2451501.5722	2.243	1.352	1.170	1.168	1.073	0.002	0.709	0.180
2451501.6023	2.235	1.356	1.168	1.170	1.067	-0.002	0.691	0.190
2451502.6026	2.240	1.355	1.176	1.176	1.064	0.000	0.706	0.179
2451503.5947	2.244	1.351	1.174	1.175	1.070	-0.001	0.716	0.178
2451504.5942	2.232	1.344	1.162	1.162	1.070	0.000	0.706	0.182
2451509.5782	2.204	1.329	1.151	1.150	1.053	0.001	0.697	0.177
2451509.5857	2.205	1.332	1.155	1.148	1.050	0.007	0.696	0.170
2451510.5704	2.207	1.329	1.150	1.146	1.057	0.004	0.699	0.175
2451510.5857	2.207	1.330	1.150	1.147	1.057	0.003	0.697	0.177
2451511.5856	2.221	1.339	1.152	1.153	1.069	-0.001	0.695	0.188
2451514.5860	2.251	1.357	1.171	1.167	1.080	0.004	0.708	0.182
2451656.9855	2.212	1.345	1.155	1.155	1.057	0.000	0.677	0.190
2451657.9781	2.215	1.342	1.161	1.151	1.054	0.010	0.692	0.171
2451658.9770	2.205	1.342	1.157	1.153	1.048	0.004	0.678	0.181
2451659.9720	2.206	1.334	1.147	1.144	1.059	0.003	0.685	0.184
2451660.9784	2.199	1.325	1.139	1.133	1.060	0.006	0.688	0.180
2451661.9866	2.185	1.318	1.133	1.124	1.052	0.009	0.682	0.176
2451663.9785	2.223	1.318	1.127	1.124	1.096	0.003	0.714	0.188
2451664.9700	2.185	1.316	1.134	1.130	1.051	0.004	0.687	0.178
2451665.9786	2.183	1.320	1.141	1.138	1.042	0.003	0.684	0.176
2451666.9701	2.184	1.327	1.144	1.144	1.040	0.000	0.674	0.183
2451667.9671	2.191	1.324	1.140	1.137	1.051	0.003	0.683	0.181
2451668.9628	2.186	1.318	1.137	1.134	1.049	0.003	0.687	0.178
2451669.9658	2.173	1.314	1.129	1.125	1.044	0.004	0.674	0.181
2451670.9425	2.167	1.308	1.127	1.125	1.040	0.002	0.678	0.179
2451671.9491	2.166	1.312	1.126	1.124	1.040	0.002	0.668	0.184
2451672.9501	2.177	1.319	1.128	1.123	1.049	0.005	0.667	0.186
2451673.9472	2.181	1.325	1.133	1.132	1.048	0.001	0.664	0.191

TABLE 2—*Continued*

HJD	u	v	b	y	$u-b$	$b-y$	c_1	m_1
2451674.9462	2.192	1.345	1.149	1.145	1.043	0.004	0.651	0.192
2451684.9161	2.181	1.318	1.140	1.138	1.041	0.002	0.685	0.176
2451689.9027	2.202	1.329	1.149	1.143	1.053	0.006	0.693	0.174
2451698.9054	2.169	1.328	1.137	1.139	1.032	-0.002	0.650	0.193
2451699.8961	2.164	1.324	1.139	1.134	1.025	0.005	0.655	0.180
2451700.9000	2.166	1.329	1.137	1.136	1.029	0.001	0.645	0.191
2451704.8900	2.214	1.354	1.158	1.153	1.056	0.005	0.664	0.191
2451705.8823	2.208	1.342	1.157	1.156	1.051	0.001	0.681	0.184
2451706.8807	2.225	1.348	1.164	1.167	1.061	-0.003	0.693	0.187
2451707.8820	2.231	1.360	1.168	1.168	1.063	0.000	0.679	0.192
2451708.8798	2.232	1.354	1.171	1.166	1.061	0.005	0.695	0.178
2451709.8760	2.231	1.360	1.174	1.171	1.057	0.003	0.685	0.183
2451710.8847	2.235	1.359	1.187	1.171	1.048	0.016	0.704	0.156
2451711.8690	2.231	1.353	1.167	1.164	1.064	0.003	0.692	0.183
2451712.8621	2.218	1.348	1.161	1.155	1.057	0.006	0.683	0.181
2451729.8198	2.169	1.304	1.122	1.130	1.047	-0.008	0.683	0.190
2451809.6045	2.198	1.327	1.148	1.149	1.050	-0.001	0.692	0.180
2451810.6860	2.197	1.330	1.145	1.148	1.052	-0.003	0.682	0.188
2451815.6754	2.215	1.357	1.175	1.177	1.040	-0.002	0.676	0.184
2451816.6651	2.220	1.360	1.183	1.176	1.037	0.007	0.683	0.170
2451817.6596	2.224	1.373	1.185	1.185	1.039	0.000	0.663	0.188
2451823.6563	2.191	1.318	1.141	1.147	1.050	-0.006	0.696	0.183
2451823.6432	2.184	1.313	1.146	1.147	1.038	-0.001	0.704	0.168
2451825.6436	2.192	1.321	1.146	1.148	1.046	-0.002	0.696	0.177
2451830.6280	2.220	1.325	1.160	1.163	1.060	-0.003	0.730	0.168
2451831.6222	2.212	1.332	1.159	1.164	1.053	-0.005	0.707	0.178
2451833.6201	2.193	1.317	1.144	1.149	1.049	-0.005	0.703	0.178
2451834.6195	2.190	1.317	1.141	1.144	1.049	-0.003	0.697	0.179
2451842.6092	2.181	1.319	1.144	1.147	1.037	-0.003	0.687	0.178
2451844.5860	2.185	1.316	1.149	1.144	1.036	0.005	0.702	0.162

TABLE 2—*Continued*

HJD	u	v	b	y	$u-b$	$b-y$	c_1	m_1
2451847.6401	2.200	1.330	1.152	1.151	1.048	0.001	0.692	0.177
2451849.5932	2.197	1.328	1.151	1.155	1.046	-0.004	0.692	0.181
2451850.5907	2.193	1.323	1.153	1.151	1.040	0.002	0.700	0.168
2451857.5724	2.187	1.311	1.146	1.149	1.041	-0.003	0.711	0.168
2451861.5700	2.201	1.329	1.162	1.164	1.039	-0.002	0.705	0.169
2451864.5691	2.192	1.328	1.153	1.153	1.039	0.000	0.689	0.175
2451867.5690	2.169	1.309	1.144	1.146	1.025	-0.002	0.695	0.167
2451869.5677	2.175	1.310	1.141	1.145	1.034	-0.004	0.696	0.173
2451874.5741	2.174	1.310	1.138	1.143	1.036	-0.005	0.692	0.177
2451875.5665	2.179	1.314	1.149	1.149	1.030	0.000	0.700	0.165
2451877.5662	2.194	1.330	1.154	1.156	1.040	-0.002	0.688	0.178
2452030.9561	2.163	1.314	1.137	1.138	1.026	-0.001	0.672	0.178
2452031.9505	2.171	1.318	1.140	1.144	1.031	-0.004	0.675	0.182
2452034.9587	2.196	1.332	1.152	1.154	1.044	-0.002	0.684	0.182
2452035.9681	2.209	1.336	1.154	1.157	1.055	-0.003	0.691	0.185
2452036.9480	2.237	1.344	1.160	1.163	1.077	-0.003	0.709	0.187
2452037.9403	2.221	1.340	1.161	1.162	1.060	-0.001	0.702	0.180
2452038.9407	2.213	1.344	1.157	1.158	1.056	-0.001	0.682	0.188
2452039.9422	2.216	1.344	1.162	1.164	1.054	-0.002	0.690	0.184
2452044.9106	2.221	1.343	1.159	1.164	1.062	-0.005	0.694	0.189
2452045.9322	2.216	1.337	1.163	1.159	1.053	0.004	0.705	0.170
2452046.9203	2.219	1.340	1.159	1.165	1.060	-0.006	0.698	0.187
2452050.8982	2.208	1.330	1.145	1.147	1.063	-0.002	0.693	0.187
2452051.9021	2.196	1.325	1.142	1.139	1.054	0.003	0.688	0.180
2452052.9008	2.193	1.321	1.134	1.138	1.059	-0.004	0.685	0.191
2452053.8872	2.184	1.320	1.136	1.134	1.048	0.002	0.680	0.182
2452055.8843	2.180	1.315	1.123	1.130	1.057	-0.007	0.673	0.199
2452058.8930	2.189	1.322	1.145	1.142	1.044	0.003	0.690	0.174
2452061.8678	2.184	1.323	1.138	1.149	1.046	-0.011	0.676	0.196
2452062.9052	2.191	1.310	1.138	1.142	1.053	-0.004	0.709	0.176

Table 2—*Continued*

HJD	u	v	b	y	$u-b$	$b-y$	c_1	m_1
2452064.8663	2.192	1.311	1.136	1.139	1.056	-0.003	0.706	0.178
2452073.8330	2.202	1.323	1.156	1.153	1.046	0.003	0.712	0.164
2452074.8332	2.200	1.313	1.151	1.155	1.049	-0.004	0.725	0.166
2452074.8305	2.193	1.318	1.149	1.149	1.044	0.000	0.706	0.169
2452076.8383	2.167	1.307	1.119	1.123	1.048	-0.004	0.672	0.192
2452084.8073	2.167	1.294	1.122	1.132	1.045	-0.010	0.701	0.182
2452087.8001	2.185	1.303	1.135	1.138	1.050	-0.003	0.714	0.171
2452088.7921	2.188	1.310	1.136	1.137	1.052	-0.001	0.704	0.175

Table 3

Strömgren Photometric Parameters derived from the data.

Filter or Color	Magnitude	Amplitude of Variability
u	2.202	0.018
v	1.331	0.016
b	1.152	0.014
y	1.149	0.014
$u-b$	1.050	0.009
$b-y$	0.003	0.005
c_1	0.692	0.017
m_1	0.177	0.010

TABLE 4

COEFFICIENTS FOR THE SINE WAVE FITS (THROUGH χ^2 MINIMIZATION) TO THE RADIAL PULSATIONS SHOWN IN FIGURE 9 AS WELL AS OTHER VARIABLES WE FITTED. THE ERRORS ARE THE STANDARD ERRORS OF THE FIT.

Season	Type	Period (days)	A (km s^{-1}) or (mag)	x_c (phase)	c (km s^{-1}) or (mag)
Fall 1998	u	17.8	-0.016 ± 0.002	0.39 ± 0.02	2.208 ± 0.001
Fall 1998	v	17.8	-0.011 ± 0.002	0.42 ± 0.04	1.335 ± 0.002
Fall 1998	b	17.8	-0.011 ± 0.002	0.38 ± 0.04	1.162 ± 0.002
Fall 1998	y	17.8	-0.011 ± 0.002	0.42 ± 0.03	1.160 ± 0.001
Fall 1998	Si II RV	17.8	2.27 ± 0.62	0.19 ± 0.03	-2.56 ± 0.43
Fall 1999	u	13.4	-0.023 ± 0.002	0.38 ± 0.02	2.211 ± 0.002
Fall 1999	v	13.4	-0.016 ± 0.002	0.39 ± 0.02	1.336 ± 0.001
Fall 1999	b	13.4	-0.017 ± 0.002	0.39 ± 0.02	1.155 ± 0.001
Fall 1999	y	13.4	-0.017 ± 0.002	0.39 ± 0.02	1.152 ± 0.001
Fall 1999	Si II RV	13.4	1.21 ± 0.57	0.17 ± 0.08	-2.76 ± 0.42

Table 5

Hot supergiant stars observed at Ritter Observatory with the same spectroscopic instrumentation as the observations presented here. All stars with an absence of the absorption events have more than 40 observations. Presented here are fundamental properties, the number of observations, and whether high velocity absorption events have been seen in our data. Kaufer et al. (1996) also found high velocity absorption in the late B-type supergiants HD 91619 and HD 96919, which both are hotter and more luminous than Deneb and are inaccessible to the instrumentation used in this survey. ν Cep is nearly identical to Deneb, but has not exhibited any high velocity absorption events.

Star	MK	$T_{\tt eff}$ K	$\log(L/L_\odot)$	Reference (Stellar Parameters)	Number of Spectra	Years of Data	Absorption Events?
Rigel	B8 Ia	12500	5.56	Markova et al. (2008)	203	1996-2007	yes
HR 8020	B8Iae	13000	5.08	Markova et al. (2008)	29	2000-2006	yes
HR 1035	B9 Ia	9730	4.92	Verdugo et al. (1999)	108	1994-2007	yes
HR 1040	A0 Ia	9600	4.76	Barlow & Cohen (1977)	187	1993-2007	yes
9 Per	A2 Ia	9000	4.99	Kudritzki et al. (1999a)	40	1993-2005	yes
Deneb	A2 Ia	8500	5.20	Aufdenberg et al. (2002)	781	1993-2007	yes, rare
ν Cep	A2 Ia	8500	4.76		119	1994-2007	no, See Footnote 3
6 Cas	A3 Ia	8400	5.13	Kudritzki et al. (1999)	69	1993-2007	no